Genetic evidence for functional diversification of gram-negative intermembrane phospholipid transporters

Ashutosh K. Rai[a], Katsuhiro Sawasato[b], Haley C. Bennett[a], Anastasiia Kozlova[b], Genevieve C. Sparagna[c], Mikhail Bogdanov[b], and Angela M. Mitchell[a,#]

[a] Department of Biology, Texas A&M University, College Station, Texas, USA

[b] Department of Biochemistry and Molecular Biology, McGovern Medical School at The University of Texas Health Science Center at Houston, Houston, Texas, USA

[c] Department of Medicine, Division of Cardiology, University of Colorado Anschutz Medical Campus, Aurora, Colorado, USA

Running title: Phospholipid transporter functional differentiation

Address correspondence to Angela M. Mitchell, amitchell@bio.tamu.edu

Keywords: phospholipid trafficking, gram-negative envelope, outer membrane, lipid metabolism, cold sensitivity

Abstract

The outer membrane of Gram-negative bacteria is a barrier to chemical and physical stress. Phospholipid transport between the inner and outer membranes has been an area of intense investigation and, in *E. coli* K-12, it has recently been shown to be mediated by YhdP, TamB, and YdbH, which are suggested to provide hydrophobic channels for phospholipid diffusion, with YhdP and TamB playing the major roles. However, YhdP and TamB have different phenotypes suggesting distinct functions. We investigated these functions using synthetic cold sensitivity (at 30 °C) caused by deletion of *yhdP* and *fadR*, a transcriptional regulator controlling fatty acid degradation and unsaturated fatty acid production, but not by Δ*tamB* Δ*fadR* or Δ*ydbH* Δ*fadR*,. Deletion of *tamB* suppresses the Δ*yhdP* Δ*fadR* cold sensitivity suggesting this phenotype is related to phospholipid transport. The Δ*yhdP* Δ*fadR* strain shows a greater increase in cardiolipin upon transfer to the non-permissive temperature and genetically lowering cardiolipin levels can suppress cold sensitivity. These data also reveal a qualitative difference between cardiolipin synthases in *E. coli*, as deletion of *clsA and clsC* suppresses cold sensitivity but deletion of *clsB* does not despite lower cardiolipin levels. In addition to increased cardiolipin, increased fatty acid saturation is necessary for cold sensitivity and lowering this level genetically or through supplementation of oleic acid suppresses the cold sensitivity of the Δ*yhdP* Δ*fadR* strain. Although indirect effects are possible, we favor the parsimonious hypothesis that YhdP and TamB have differential substrate transport preferences, most likely with YhdP preferentially transporting more saturated phospholipids and TamB preferentially transporting more unsaturated phospholipids. We envision cardiolipin contributing to this transport preference by sterically clogging TamB-mediated transport of saturated phospholipids. Thus, our data provide a potential mechanism for independent control of the phospholipid composition of the inner and outer membranes in response to changing conditions.

Author Summary

Gram-negative bacteria possess a highly impermeable outer membrane, which protects against environmental stress and antibiotics. Outer membrane phospholipid transport remained mysterious until YhdP, TamB, and YdbH were recently implicated in phospholipid transport between the inner and outer membranes of *E. coli*. Similar roles for YhdP and/or TamB have been suggested in both closely and distantly related gram-negative bacteria. Here, given the transporters' apparent partial redundancy, we investigated functional differentiation between YhdP and TamB. Our data suggest YhdP and TamB have differential involvement with fatty acid and phospholipid metabolism. In fact, transport of higher than normal levels of cardiolipin and saturated phospholipids in the absence of YhdP and presence of TamB at a non-permissive temperature is lethal. We suggest a model where the functions of YhdP and TamB are distinguished by phospholipid transport preference with YhdP preferentially transporting more saturated phospholipids and TamB more unsaturated phospholipids. Cardiolipin headgroup specificity may contribute transport inhibition due to its bulky nature inhibiting the passage of other phospholipids. Diversification of function between YhdP and TamB provides a mechanism for regulation of phospholipid composition, and possibly the mechanical strength and permeability of the outer membrane, and so the cell's intrinsic antibiotic resistance, in changing environmental conditions.

Introduction

The gram-negative bacterial cell envelope has an outer membrane (OM) that sits outside the aqueous periplasm and peptidoglycan cell wall. The OM provides a barrier against various environmental stresses including toxic molecules such as antibiotics and osmotic pressure (1-6). Unlike the inner membrane (IM), a phospholipid bilayer, the OM is largely composed of phospholipids (mainly phosphatidylethanolamine (PE) (7)) in its inner leaflet and LPS (lipopolysaccharide) in its outer leaflet (2, 8). However, both membranes are asymmetric as the IM has different phospholipid compositions in its inner versus outer leaflets (9). Outer membrane proteins (OMPs) form a network across the cell surface interspersed with phase separated LPS patches (10). Lipoproteins are generally anchored in the inner (i.e., periplasmic) leaflet of the OM (11).

OM components are synthesized in the cytoplasm or IM and transported to the OM. OMP (12), lipoprotein (11), and LPS (13) transport pathways are well defined. However, until recently, intermembrane phospholipid transport (between the IM and OM), especially anterograde transport from the IM to the OM, has remained very poorly understood. Phospholipids are synthesized at the IM's inner leaflet (14) and rapid, bidirectional intermembrane phospholipid transport occurs (15), even without ATP (16). Phospholipid transport has a relaxed specificity, allowing transport of non-native lipids (17, 18); however, intermembrane phospholipid composition differences are maintained (7, 19-22). For instance, the OM is enriched for PE and its saturated species compared to the IM outer leaflet (7, 9, 20-22); however, phosphatidylglycerol (PG) and cardiolipin (CL) can be evenly distributed between the IM and OM when the cellular level of PE is greatly reduced (17), suggesting a maintenance of membrane charge balance. This headgroup redistribution is accompanied by a concomitant fatty acid redistribution evidenced by an accumulation of palmitic acid (C16:0) and cyclopropane derivatives of palmitoleic acid (C16:1) and *cis*-vaccenic acid (C18:1). In contrast, the 1,2-diglyceride that accumulates in mutants lacking DgkA (diglyceride kinase) predominantly associates with the IM (23), suggesting existence of a mechanism of discrimination of lipid transfer to the OM that does not recognize diglyceride molecules and contributes to the diversification of distribution of polar and acyl groups between the IM and OM. This establishment and maintenance of defined lipid topography between the IM and the OM must involve the coordinated biosynthesis and balanced bidirectional trafficking of specific phospholipids across the IM and from the IM to the OM (24).

It has been demonstrated that anterograde phospholipid transport is mediated by a high-flux, diffusive (i.e., concentration gradient, not energy dependent) system in *Escherichia coli* (25). A retrograde trafficking pathway, the Mla system, removes mislocalized phospholipids from the OM outer leaflet and returns them to the IM (26). A gain-of-function allele, *mlaA** (27, 28), opens a channel allowing phospholipids to mislocalize to the cell surface by flowing from the OM's inner to outer leaflet (27, 29), resulting in a PldA (OM phospholipase A)-mediated attempt to reestablish OM asymmetry by increasing LPS

112 production, OM vesiculation, and increased flow of phospholipids to the OM (27, 28).
113 When nutrients are depleted, inhibiting phospholipid production, cells lyse due to loss of
114 IM integrity (16, 18). Single cell imaging of *mlaA** cells confirmed an aberrant lipid flow
115 from the IM to the OM at a fast rate. Loss of YhdP, an inner membrane protein, could
116 significantly slow phospholipid flow to the OM resulting in loss of OM integrity before IM
117 rupture (25), suggesting YhdP might play a role in intermembrane phospholipid transport.

118 Recently, YhdP and two homologs, TamB and YdbH, were demonstrated to be
119 intermembrane phospholipid transporters (30, 31). Ruiz, *et al*. investigated AsmA family
120 proteins and found Δ*yhdP* Δ*tamB* mutants showed synthetic OM permeability and
121 stationary phase lysis (30). Moreover, when combined, Δ*yhdP*, Δ*tamB*, and Δ*ydbH* are
122 synthetically lethal. Genetic interactions of these mutants with *mlaA* and *pldA* show their
123 involvement in OM phospholipid homeostasis. Predicted structures of YhdP, TamB, and
124 YdbH (32, 33), as well as a partial crystal structure of TamB (34), have a β-taco fold domain
125 with a hydrophobic pocket, resembling eukaryotic lipid transporters (35-38). These
126 structural findings are another clue that suggests YhdP, TamB, and YdbH are involved in
127 phospholipid transport. Douglass, *et al.* confirmed the synthetic lethality of Δ*yhdP*,
128 Δ*tamB*, and Δ*ydbH* and demonstrated a Δ*tamB* Δ*ydbH* mutant with reduced *yhdP*
129 expression had decreased amounts of OM phospholipids, directly demonstrating their
130 involvement in intermembrane phospholipid transport or its regulation (31). Structural
131 studies have shown that YhdP is long enough to span the periplasmic space and molecular
132 dynamics indicate that the C-terminus of YhdP can insert into the OM to allow
133 phospholipid transfer between the membranes (39). This study also directly
134 demonstrates that a phosphate containing substrate, putatively assigned to be
135 phospholipids, can be crosslinked to the hydrophobic groove of YhdP (39). The role of
136 YhdP, TamB, and YdbH in phospholipid transport may be widely conserved as recent
137 evidence implicates TamB in anterograde phospholipid transport in *Veillonella parvula*, a
138 diderm Fermicute (40) and YhdP, TamB, YdbH, and PA4735 in intermembrane
139 phospholipid transport in *Pseudomonas aeruginosa* (41).

140 Nevertheless, why there are three separate intermembrane phospholipid transport
141 proteins and the functional interactions between these proteins remains unanswered,
142 although it is clear the proteins are not fully redundant or functionally equivalent. The
143 conditional expression of *yhdP* alone, without the presence of *ydbH* and *tamB*, fully
144 complements neither growth phenotypes nor a normal level of OM phospholipids,
145 suggesting transport function is still impaired in this strain (31). In addition, YdbH seems
146 to play a more minor role than YhdP and TamB (30, 31) and the screen identifying Δ*yhdP*
147 as slowing *mlaA**-dependent lysis did not identify Δ*tamB* or Δ*ydbH* (25). Moreover, we
148 previously identified a role for YhdP in stationary phase SDS (sodium dodecyl sulfate)
149 resistance and modulating cyclic enterobacterial common antigen activity (42, 43) not
150 shared by TamB and YdbH (**Fig. S1AB**) (30, 31, 42, 43). Similarly, TamB, in conjunction with

151 TamA, has been suggested to play a role in OM insertion of some "complicated" β-barrel
152 OMPs such as autotransporters and usher proteins (34, 44-46).

153 Here, we investigated the differentiation of YhdP and TamB function and identified
154 synthetic cold sensitivity in a strain with Δ*yhdP* and Δ*fadR*, a transcriptional regulator of
155 fatty acid biosynthesis and degradation, acting as a transcriptional switch between these
156 pathways in response to acyl-CoA (47). FadR is necessary for normal levels of unsaturated
157 fatty acids to be synthesized (48). The cold sensitivity was unique to the Δ*yhdP* Δ*fadR*
158 strain and was suppressed by loss of TamB, demonstrating that the sensitivity is related
159 to phospholipid transport. We found that the Δ*yhdP* Δ*fadR* mutant had a greater increase
160 in levels of a specific phospholipid, cardiolipin (CL) during growth at the non-permissive
161 temperature, and decreasing CL suppressed cold sensitivity. Furthermore, increasing
162 unsaturated fatty acid levels suppressed cold sensitivity. Overall, our data are consistent
163 with a model where TamB and YhdP transport functions are differentiated based on
164 phospholipid fatty acid saturation state, with TamB transporting more unsaturated
165 phospholipids and YhdP transporting more saturated phospholipids, although indirect
166 effects may contribute to the phenotype. Phospholipid species or head group can also
167 contribute to transport specificity, since higher levels of dianionic CL are necessary for the
168 cold sensitivity phenotype, potentially due to functional inhibition of TamB by clogging of
169 its hydrophobic groove.

170

171

172 **Results**

173 **Loss of FadR and YhdP results in cold sensitivity suppressed by loss of TamB.** To
174 investigate YhdP-TamB function differentiation, we created a Δ*yhdP* Δ*fadR* strain, as FadR
175 is a major regulator of lipid homeostasis (47). A deletion strain of *fadR* alone is expected
176 to have decreased fatty acid synthesis, increased fatty acid degradation, and increased
177 fatty acid saturation (47, 48). Surprisingly, Δ*yhdP* Δ*fadR* cultures grown at 30 °C lagged for
178 more than 8 hours, followed by highly variable growth, suggesting suppressor outgrowth
179 (**Fig.1A**). The growth defect was decreased at 37 °C and completely absent at 42 °C. To
180 confirm this cold sensitivity, we estimated efficiency of plating (EOP) and confirmed the
181 severe cold intolerance of the Δ*yhdP* Δ*fadR* strain (5 logs at 30 °C and 3 logs at 37 °C) (**Fig.
182 1B**). Although, enterobacterial common antigen is necessary for Δ*yhdP*'s OM permeability
183 phenotypes (43), the Δ*yhdP* Δ*fadR* strain's cold sensitivity was unchanged when
184 enterobacterial common antigen was not present (Δ*wecA*) (49) (**Fig. 1C**).

185 We hypothesized the Δ*yhdP* Δ*fadR* strain's cold sensitivity was due to impairment of
186 phospholipid transport and expected Δ*tamB* and/or Δ*ydbH* to show similar synthetic
187 phenotypes with Δ*fadR*. However, Δ*fadR* Δ*tamB* and Δ*fadR* Δ*ydbH* strains had no growth
188 defects (**Fig 1D**). Although Δ*ydbH* in the Δ*yhdP* Δ*fadR* strain did not alter cold sensitivity
189 (**Fig. 1E**), Δ*tamB* in the Δ*yhdP* Δ*fadR* background completely suppressed the cold
190 sensitivity (**Fig. 1F**). Consistent with previous observations for Δ*yhdP* Δ*tamB* (30), the

191 Δ*yhdP* Δ*fadR* Δ*tamB* strain was mucoid due to Rcs (regulator of capsule synthesis) stress
192 response activation and colanic acid capsule production. Deleting *rcsB*, an Rcs response
193 regulator, prevented mucoidy but did not affect suppression (**Fig. 1F**). We observed only
194 minimal growth phenotypes at 30 °C in the Δ*yhdP* Δ*fadR* Δ*tamB* strain (**Fig. 1G**), similar to
195 those of Δ*yhdP* Δ*tamB* (**Fig. S1C**). Thus, although Δ*fadR* does not suppress Δ*yhdP* Δ*tamB*
196 phenotypes, these data make slow growth an unlikely suppression mechanism. Together,
197 these data suggest the Δ*yhdP* Δ*fadR* strain has impaired phospholipid transport leading
198 synthetic cold sensitivity, which can be relieved by deletion of Δ*tamB*, shifting
199 phospholipid transport to YdbH or causing some regulatory change.

200 We next looked for envelope homeostasis alterations in the Δ*yhdP* Δ*fadR* strain. To
201 identify cell lysis and/or severe OM permeability defects at 30 °C, we assayed CPRG
202 (chlorophenol red-β-D-galactopyranoside) processing. CPRG must contact LacZ in the
203 cytoplasm or supernatant to release chlorophenol red (50). Compared to wild type or
204 single mutants, the Δ*yhdP* Δ*fadR* strain had increased CPRG processing (**Fig. S2A**),
205 demonstrating lysis or increased envelope permeability. When we assayed resistance to
206 molecules excluded by the OM (1, 42, 43, 51, 52) at 37 °C, a semi-permissive temperature,
207 the Δ*yhdP* Δ*fadR* strain showed sensitivity to vancomycin, a large scaffold antibiotic, and
208 SDS EDTA compared to single mutants (**Fig. S2B**). However, with bacitracin treatment or
209 EDTA treatment alone, the Δ*yhdP* Δ*fadR* strain phenocopied the Δ*fadR* single deletion
210 (**Fig. S2CD**). LPS levels were not altered in the Δ*yhdP*, Δ*fadR*, Δ*yhdP* Δ*fadR* or Δ*yhdP* Δ*fadR*
211 Δ*tamB* strains (**Fig. S2E**). OM asymmetry mutations (i.e., Δ*pldA*, Δ*mlaA*) (26-28, 53) did
212 not have suppressive or synthetic effects on cold sensitivity in the Δ*yhdP* Δ*fadR* strain (**Fig.**
213 **S3AB**), cold sensitivity is not due to OM asymmetry or the loss thereof. Overall, the
214 changes in OM permeability did not seem sufficient to cause lethality at lower
215 temperature, suggesting the phospholipid transport disruption affects both IM and OM
216 integrity.

217 **Lowering cardiolipin suppresses cold sensitivity.** We investigated phospholipid
218 composition of the wild-type, Δ*yhdP*, Δ*fadR*, and Δ*yhdP* Δ*fadR* strains grown at the
219 permissive temperature (42 °C) to log phase then downshifted to 30 °C. *E. coli*
220 phospholipid composition is generally 75% phosphatidylethanolamine (PE), 20%
221 phosphatidylglycerol (PG), and 5% cardiolipin (CL) with CL increasing in stationary phase
222 (14, 54). Of the three CL synthases, ClsA and ClsB synthesize CL from two PG molecules,
223 while ClsC synthesizes CL from one PG and one PE molecule, so CL and PG levels are
224 generally reciprocally regulated (55-58). For all strains, the levels of PE were similar (**Fig.**
225 **2A**, **Fig. S4A**). However, the Δ*yhdP* Δ*fadR* strain had increased CL and concomitant
226 decreased PG compared to the wild-type strain and compared to individual Δ*yhdP* and
227 Δ*fadR* mutants (**Fig. 2B**). PgsA synthesizes phosphatidylglycerol-phosphate and is the first
228 enzyme differentiating PG and PE biosynthesis. PgsA depletion would decrease both PG
229 and CL levels, reversing increased CL levels and exacerbating decreased PG levels in the
230 Δ*yhdP* Δ*fadR* strain. We tested the effect of PgsA depletion in a strain background (Δ*rcsF*
231 Δ*lpp*) where *pgsA* is non-essential (59-62). When *pgsA* expression was repressed (glucose

panel), the Δ*yhdP* Δ*fadR* cold sensitivity was partially suppressed (**Fig. 2C**), demonstrating that decreased PG does not cause cold sensitivity and suggesting increased CL may be necessary for cold sensitivity. The partial suppression may be due to incomplete depletion of PG and CL or the adaptive response of a cell containing only PE in its membrane. Induction of *pgsA* (arabinose panel) reversed the suppression. The cold sensitivity of the Δ*yhdP* Δ*fadR* strain was lost when CL was fully depleted due to deletion of the genes for all cardiolipin syntheses (Δ*clsABC*) or of the gene for the primary cardiolipin synthase (Δ*clsA*) responsible for CL synthesis in exponential phase (**Fig. 2ADE**, **Fig. S4B**). A decrease in LPS levels is not responsible for the suppression as LPS levels did not change in the Δ*yhdP* Δ*fadR* Δ*clsA* strain (Δ*yhdP* Δ*fadR* Δ*tamB*). Δ*clsB* caused a smaller decrease in CL levels, while Δ*clsC* did not cause a decrease (**Fig. 2AB**, **Fig. 4B**). Surprisingly, however, Δ*clsC* completely suppressed the cold sensitivity, while Δ*clsB* did not (**Fig. 2FG**). Thus, increased CL is necessary for cold sensitivity but CL levels alone cannot explain the phenotype: another factor, such as a specific molecular form (e.g., acyl chain length, saturation state, symmetry of acyl chain arrangement) or localization (e.g., poles vs. midcell or inner vs. outer leaflet) of CL, is required.

Increased *fabA* expression suppresses cold sensitivity. To identify other factors involved in the cold sensitivity, we applied a forward genetic approach by isolating spontaneous suppressor mutants capable of growing at 30 °C and identified a suppressor mutant (Suppressor 1) that restored growth at 30 °C (**Fig. 3A**), decreased CPRG processing (**Fig. S2A**), and had very similar CL levels (**Fig. 2AB**, **Fig. S4A**) and LPS levels (**Fig. S2**) to the Δ*yhdP* Δ*fadR* strain. We identified a point mutation in the *fabA* promoter region in Suppressor 1 (**Fig. 3B**) and confirmed this mutation was sufficient for suppression (**Fig. 3C**). FabA is a dehydratase/isomerase that introduces *cis* unsaturation into fatty acids (14, 63) and *fabA* is expressed from two promoters controlled by FadR and FabR (64, 65). FadR activates *fabA* expression, while FabR represses. Thus, *fadR* deletion would be expected to lower *fabA* expression. The suppressor mutation was located in the *fabA* promoter FabR binding site (**Fig. 3B**) and we hypothesized this mutation would increase *fabA* expression. *fabA* mRNA levels were more than 4-fold lower in the Δ*yhdP* Δ*fadR* strain than the wild-type strain (**Fig. 3D**). While lower than wild type, the suppressor mutant increased *fabA* mRNA 1.6-fold over the Δ*yhdP* Δ*fadR* strain.

We constructed luciferase reporter plasmids with the wild-type *fabA* promoter region or the *fabA* promoter region containing the suppressor mutation. The reporter with the mutated promoter had higher activity in a wild-type, Δ*fadR,* and Δ*fabR* background (**Fig. 3E**). *fabA* transcription occurs from a promoter downstream of the FabR binding site (65-67). However, when *fadR* is deleted, transcription shifts to the FabR-regulated promoter within the FabR binding region (65-67). Thus, our data indicate the Suppressor 1 mutation regulates the constitutive activity of the promoter located in the FabR binding site rather than the affinity of FabR binding. To confirm the effect of changing the second promoter's activity, we tested the effect of Δ*fabR* on cold sensitivity in the Δ*yhdP* Δ*fadR* strain and observed partial suppression (**Fig. S5**). The smaller effect of Δ*fabR* compared to

273 Suppressor 1 may result from other gene expression changes or to the smaller relative
274 effect of Δ*fabR* on *fabA* expression (**Fig. 3E**). Overall, these data demonstrate increasing
275 *fabA* expression, which is necessary for unsaturated fatty acid biosynthesis, rescues cold
276 sensitivity in the Δ*yhdP* Δ*fadR* strain without changing CL levels.

277 **Increasing unsaturated fatty acids relieves cold sensitivity.** Given the effect of *fabA*
278 expression on the Δ*yhdP* Δ*fadR* cold sensitivity, we used liquid chromatography-
279 electrospray ionization mass spectrometry (LC/MS) to characterize the strains'
280 phospholipid saturation state (**Dataset S1**, **Fig. 4A-C, Fig. S6**). Representative spectra
281 demonstrating relative phospholipid composition are shown in **Fig. S7**. As expected,
282 Δ*fadR* caused increased fully saturated and monounsaturated PE and PG with a
283 concomitant decrease of diunsaturated PE (**Fig. 4AB, S6AB**). Similarly, the Δ*fadR* strain
284 demonstrated increased monounsaturated CL with a concomitant decrease in
285 triunsaturated CL (**Fig. 4C, S6C**). Compared to the Δ*fadR* strain, the Δ*yhdP* Δ*fadR* strain
286 had slightly decreased saturation for all three phospholipids, while still displaying more
287 phospholipid saturation than wild type or Δ*yhdP* strains (**Fig. 4A-C, S6C**). Suppressor 1
288 trended towards decreased saturation of all three phospholipids compared to the Δ*yhdP*
289 Δ*fadR* strain (**Fig. 4A-C, S6C**). We wondered whether the suppression difference between
290 Δ*clsC* and Δ*clsB* resulted from the CL saturation state. However, the Δ*yhdP* Δ*fadR* Δ*clsB*
291 and Δ*yhdP* Δ*fadR* Δ*clsC* strains had very similar CL profiles (**Fig. 4C, S6C**), suggesting
292 another qualitative difference affecting suppression, perhaps CL lateral or inter-leaflet
293 distribution in the cell. These strains also showed similar PE and PG saturation profiles to
294 their Δ*yhdP* Δ*fadR* parent (**Fig. 4AB, S6AB**).

295 We hypothesized increasing unsaturated fatty acids suppresses Δ*yhdP* Δ*fadR* cold
296 sensitivity and performed EOPs for cold sensitivity on media containing an unsaturated
297 fatty acid (oleic acid, C18:1 *cis*-9). Exogenous phospholipids can be taken up by *E. coli*,
298 attached to acyl-CoA, and incorporated into phospholipids (68). Oleic acid addition
299 suppressed the Δ*yhdP* Δ*fadR* strain's cold sensitivity (**Fig. 4D**). Supplementing oleic acid
300 increases unsaturated phospholipids and provides an exogenous fatty acid source. To
301 differentiate between saturation state and fatty acid availability, we compared treatment
302 with oleic acid and saturated stearic acid (C18:0). Only oleic acid, and not stearic acid,
303 suppressed the Δ*yhdP* Δ*fadR* strain's cold sensitivity (**Fig. 4E**), confirming increasing
304 unsaturated fatty acids, not fatty acid availability suppresses.

305 **Suppression causes fatty acid metabolism and stress response alterations.** In wild-type
306 cells, *fabA* overexpression does not change phospholipid saturation levels, demonstrating
307 the FabB enzyme is rate limiting for unsaturated fatty acid biosynthesis (69). We were
308 intrigued that Suppressor 1 altered saturation without directly effecting *fabB* expression.
309 We also wondered whether CL levels in the Δ*yhdP* Δ*fadR* strain are transcriptionally
310 regulated. Thus, we investigated the transcriptional landscape of the wild type, the Δ*yhdP*
311 Δ*fadR*, and Suppressor 1 strains after a 30-minute downshift of growth to 30 °C to
312 determine: (i) whether the Δ*yhdP* Δ*fadR* strain had altered *cls* gene expression; (ii)

313 whether Suppressor 1 had other transcriptional changes; and (iii) why increased *fabA*
314 expression decreased saturation. All differentially expressed genes (>2-fold change,
315 p<0.05) are listed in **Dataset S2**. Principle component analysis of these genes showed the
316 closest relation between Δ*yhdP* Δ*fadR* strain and Suppressor 1, while the wild-type strain
317 was more distantly related (**Fig. 5A**, **S8A**). Nevertheless, Suppressor 1 was more closely
318 related to wild type than was the Δ*yhdP* Δ*fadR* strain. Most differentially regulated genes
319 between Δ*yhdP* Δ*fadR* and wild type and Suppressor 1 and wild type were upregulated
320 (**Fig. 5BC**, **S8BC**). Many of the most highly regulated genes are FadR-regulon members.
321 The majority of differentially regulated genes in Suppressor 1 compared to Δ*yhdP* Δ*fadR*
322 are downregulated (**Fig. 5D, S8D**). These genes are involved in many cellular pathways
323 and likely reflect the decreased cellular stress (**Table S2**). Indeed, many external stress
324 response genes are more enriched in Δ*yhdP* Δ*fadR* than in Suppressor 1 (**Fig. S9A**).

325 No significant expression changes occurred in the CL biosynthesis pathway (**Fig. 5E**) or
326 other phospholipid biosynthesis genes (**Fig. S9B**). The increased cardiolipin in Δ*yhdP*
327 Δ*fadR* and Suppressor 1 may be post-transcriptional or due to a change in a regulatory
328 pathway not yet altered after 30 minutes at 30 °C (**Fig. S9C**). Levels of mitochondrial CL
329 can be altered due to differences in substrate binding affinity of the CL synthase based on
330 saturation, with increased saturation decreasing CL synthesis (70), and it may be that a
331 similar pathway operates here, albeit in a different direction. We examined the
332 expression of genes in fatty acid synthesis and degradation, many of which are members
333 of the FadR regulon. In Δ*yhdP* Δ*fadR* compared to wild type, many fatty acid biosynthesis
334 genes significantly decreased while many fatty acid degradation genes significantly
335 increased (**Fig. 5F**), consistent with Δ*fadR* effects. While *fabA* expression is decreased,
336 *fabB* expression is not changed, explaining why increased *fabA* expression causes
337 decreased saturation in Suppressor 1. Overall, our data demonstrate the Δ*yhdP* Δ*fadR*
338 strain's cold sensitivity is due to impaired phospholipid trafficking, and increased
339 phospholipid saturation and cardiolipin are necessary for this functional impairment.

340

341

342 **Discussion**

343 The identification of YhdP, TamB, and YdbH as putative intermembrane phospholipid
344 transporters (30, 31) posed the tantalizing question: why is having three transporters
345 advantageous? Differential phenotypes between the transporters suggest that they
346 possess specialized functions (25, 30, 31, 34, 43-46). Here, we demonstrate each protein
347 plays a distinguishable role in phospholipid transport that can be differentiated based on
348 genetic interactions with lipid metabolism. Disruption of *fadR* and *yhdP* function causes
349 synthetic cold sensitivity not shared by *tamB* or *ydbH*. This sensitivity can be suppressed
350 by removing TamB. This phenotype involves both increased levels of CL and saturated
351 fatty acids, and decreasing amounts of either suppresses. In addition, our data
352 demonstrate that CL synthesized by ClsB and ClsC is qualitatively different—resulting in
353 differential suppression phenotypes—likely due to differences in CL localization, CL-

354 mediated, leaflet-specific changes in lipid packing order (9, 24), localized membrane
355 fluidity (71), or phospholipid transporter interaction.

356 Based on the currently available data, we cannot rule out the possibility that the
357 suppressors we have identified for the Δ*yhdP* Δ*fadR* cold sensitivity act indirectly (e.g.,
358 through regulatory or adaptive changes). However, we now suggest a simple model for
359 the differentiation of function between YhdP and TamB that fully explains our data
360 without invoking additional, more complex interpretations (**Fig. 6A-C**). In this hypothesis,
361 the functions of YhdP and TamB are diversified based on the acyl carbon saturation level
362 preference of the phospholipids they transport: YhdP transports mainly phospholipids
363 with more saturated fatty acids, while TamB transports phospholipids with more
364 unsaturated fatty acids (**Fig. 6A**). Our data and previous data (30, 31) agree YdbH plays a
365 relatively minor role. In the Δ*yhdP* Δ*fadR* strain, YhdP's absence forces more saturated
366 phospholipids to be transported by TamB. At 30 °C, TamB becomes "clogged" by
367 phospholipids having more saturated fatty acyl side chains, impeding transport (**Fig. 6B**).
368 Bulky and intrinsically disordered CL molecules could contribute to the clogging sterically
369 by obstructing the lipid channel and precluding it from translocating other lipid substrates
370 (i.e., PE). We find it interesting that the phenotype of the Δ*yhdP* Δ*fadR* strain is most
371 severe at low temperature, leading to cold sensitivity. This cold-specific effect may occur
372 due to (i) temperature-dependent decreased membrane fluidity and higher lipid packing
373 order involving lower expression of FabF, which is responsible for increased diunsaturated
374 phospholipids at lower temperature (**Fig. 5F**, **Dataset 3**)(14); (ii) higher relative levels of
375 CL (72); (iii) higher amounts of per cell phospholipids at lower temperatures (72)
376 contributing to increased diffusive flow rate; or, (iv) to thermodynamic properties altering
377 TamB transport specificity and/or substrate behavior contributing to efficiency of
378 substrate loading or transport.

379 One interesting aspect of our data is that the presence of TamB, with perhaps inhibited
380 function, causes a worse phenotype than the absence of TamB. Furthermore, the
381 phenotype of a Δ*yhdP* Δ*fadR* Δ*ydbH* strain is not measurably worse than that of the Δ*yhdP*
382 Δ*fadR* strain. Together, these data suggest that YdbH is able to successfully transport
383 phospholipids in the Δ*yhdP* Δ*fadR* strain only when TamB is absent. There are several
384 possible mechanisms for this. The first is that YhdP and TamB are the primary transporters
385 and are the preferred interaction partners for other, as of yet unidentified interaction
386 partners (e.g., putative IM proteins facilitating phospholipid transfer to YhdP and TamB).
387 Another possibility is that there is direct toxicity caused by TamB clogging, perhaps
388 through leaking of micellar phospholipids into the periplasm or through stress response
389 overactivation. A third possibility is that YdbH levels are insufficient in the presence of
390 YhdP and TamB to facilitate phospholipid transport and *ydbH* is upregulated in the
391 absence of the other phospholipid transporters. This will be an interesting area for future
392 investigations.

393 Several pieces of evidence suggest dysregulation of phospholipid transport not just
394 changes to OM phospholipid composition, and so permeability or physical strength, cause
395 the cold sensitivity phenotype of the Δ*yhdP* Δ*fadR* strain. First, the cold sensitivity is
396 unaffected by removing enterobacterial common antigen, which suppresses the
397 membrane permeability of a Δ*yhdP* strain (**Fig. 1C**, (43)), and the OM permeability
398 phenotypes of the Δ*yhdP* Δ*fadR* are not severe (**Fig. S2**). Second, the cold sensitivity is
399 suppressed by deletion of Δ*tamB* (**Fig. 1FG**). Δ*yhdP* Δ*tamB* strains have much greater OM
400 permeability (30) than the Δ*yhdP* or Δ*yhdP* Δ*fadR* strains. Third, CL has been shown to
401 have a normalizing, bidirectional, and leaflet-specific effect on lipid packing order (9, 73-
402 76) and membrane fluidity (77-80) opposite of or similar to that of cholesterol,
403 respectively, and so is unlikely to contribute to a phenotype dependent solely on OM
404 membrane fluidity. Thus, the cold sensitivity phenotype correlates with the impairment
405 of phospholipid trafficking and the likely imbalance of phospholipids between the IM and
406 OM and not with the permeability phenotypes of the OM. Nonetheless, it will be useful
407 in the future to conduction comparative analysis of the phospholipid composition of pure
408 IM and OM extracts (i.e., without cross contamination of the other membrane) at both
409 permissive and non-permissive temperatures to directly link the cold sensitivity observed
410 here with changes in phospholipid transport.

411 Although both fatty acid saturation and CL levels affect the Δ*yhdP* Δ*fadR* strain's cold
412 sensitivity, evidence points to saturation rather than headgroup as the main factor
413 separating YhdP and TamB function. Specifically, YhdP loss slows phospholipid transport
414 from the IM to the OM in a *mlaA** mutant, which loses OM material due to vesiculation
415 and lysis when phospholipid biosynthesis is insufficient to replace lost phospholipids (25,
416 27). CL only accounts for 5% of phospholipids in exponentially growing cells making it
417 unlikely that the loss of CL transport could slow net phospholipid transport to the extent
418 required to slow lysis.

419 Our model suggests the IM and OM saturation state could be independently regulated
420 based on YhdP and TamB activity or levels. IM saturation is regulated by altering the
421 composition of newly synthesized fatty acids, while OM saturation could be separately
422 regulated by allowing increased transport of more saturated or unsaturated
423 phospholipids as necessary. IM and OM acyl saturation has been studied in several strains
424 of *E. coli* and in *Yersinia pseudotuberculosis* (7, 19-21) and higher saturated fatty acid
425 levels were observed in the OM than in the IM, supporting discrimination of phospholipid
426 transport based on saturation. The IM needs to maintain an appropriate level of fluidity
427 to allow IM proteins to fold and diffuse, to allow diffusion of hydrophobic molecules, to
428 regulate cellular respiration, and to maintain membrane integrity (84, 85). However, the
429 OM is a permeability barrier, a load-bearing element that resists turgor pressure (1-6),
430 and has an outer leaflet consisting of LPS (2, 8). LPS has saturated acyl chains and is largely
431 immobile in *E. coli* (86) and a specific phospholipid saturation level may be necessary to
432 match or counterbalance LPS rigidity. OM phospholipids may also play a role in the

433 physical strength of the membrane. Interestingly, previous work has demonstrated that
434 the tensile strength of the OM is lessened in a *yhdP* mutant (25).

435 Possessing two different phospholipid transporters with different saturation state
436 preferences would allow the cell to adapt OM saturation to changing conditions including
437 temperature shifts, chemical and physical insults, or changes in synthesis of other OM
438 components (e.g., LPS or OMPs). A recent study demonstrated in *Y. pseudotuberculosis*
439 the difference in saturation levels between the membranes is exaggerated at 37 °C
440 compared to 8 °C (21). Thus, conditions where IM and OM saturation are independently
441 regulated exist and this regulation is likely important for optimum fitness of the cells.
442 Transcriptional regulation of *yhdP* and *tamB* has not been thoroughly explored. It seems
443 likely *yhdP* transcription is quite complex with several promoters and transcriptional
444 termination sites (87-89). *tamB* is predicted to be in an operon with *tamA* (which codes
445 for an OMP necessary for TamB function) and *ytfP* (87, 90) and to have a σ^E-dependent
446 promoter (91). The σ^E stress response is activated by unfolded OMP accumulation, and
447 downregulates the production of OMPs and upregulates chaperones and folding
448 machinery (74). It is intriguing to speculate a change in OM phospholipid composition
449 might aid in OMP folding due to altered biophysical properties and/or lipoprotein
450 diffusion. In fact, this could explain the observations that some complicated OMPs fold
451 more slowly in the absence of TamB (34, 44-46). Proper phospholipid composition may
452 be necessary for efficient folding of these OMPs, as it is necessary for the correct folding
453 and topology of some IM proteins (73, 92-95). Recently, it has been demonstrated that
454 the *tamAB* operon is regulated by PhoPQ in *Salmonella enterica* Serovar Typhimurium
455 and that this regulation helps maintain OM integrity in the acidic phagosome
456 environment, perhaps due to indirect effects on OMP folding (96). Thus, changing
457 environments may necessitate changes in phospholipid composition that can be
458 accomplished through differential TamB and, perhaps YhdP, regulation.

459 The mechanism of phospholipid transfer between the IM and OM has been one of the
460 largest remaining questions in gram-negative envelope biogenesis and has remained an
461 area of intense investigation for decades. Furthermore, given the lack of knowledge of
462 this pathway, the role of phospholipid composition in the permeability barrier of the OM,
463 and so the intrinsic antibiotic resistance of gram-negative bacteria, remains unknown.
464 Recent work has begun to elucidate the intermembrane phospholipid transport pathway
465 by identifying YhdP, TamB, and YdbH as proteins capable of transporting phospholipids
466 between the membranes (25, 30, 31). Our work here suggests that YhdP and TamB may
467 have separate roles in phospholipid transport that are differentiated by their preference
468 for phospholipid saturation states and possibly lipid headgroup. Homologs of YhdP and
469 TamB are found throughout *Enterobacterales* and more distantly related members of the
470 AsmA family are widespread in gram-negative bacteria (97). In fact, TamB has recently
471 been shown to play a role in anterograde intermembrane phospholipid transport in the
472 diderm Firmicute *Veillonella parvula* (40, 98) and four AsmA members play a role in
473 phospholipid transport in *Pseudomonas aeruginosa* (41). Structural predictions of YhdP

474 and TamB are strikingly similar between species (32, 33). Given this, it is quite likely similar
475 mechanisms of discrimination in intermembrane phospholipid transfer exist in other
476 species. The data we present here provide a framework for investigation of phospholipid
477 transport and mechanisms differentiating phospholipid transporter function in these
478 species.
479
480
481 **Materials and Methods**

482 **Bacterial strains and Growth Conditions. Table S3** lists the strains used in this study. Most
483 knockout strains were constructed with Keio collection alleles using P1vir transduction
484 (99, 100). New alleles were constructed through λ-red recombineering (101), using the
485 primers indicated in **Table S4**. The FLP recombinase-FRT system was used to remove
486 antibiotic resistance cassettes as has been described (101). *E. coli* cultures were grown in
487 LB Lennox media at 42°C, unless otherwise mentioned. Where noted, LB was
488 supplemented with vancomycin (Gold Biotechnology), bacitracin (Gold Biotechnology),
489 SDS (Thermo Fisher Scientific), EDTA (Thermo Fisher Scientific), oleic acid (Sigma Aldrich),
490 stearic acid (Sigma Aldrich), arabinose (Gold Biotechnology), or glucose (Thermo
491 Scientific). For plasmid maintenance, media was supplemented with 25 µg/mL kanamycin
492 (Gold Biotechnology), 10 or 20 µg/mL chloramphenicol (Gold Biotechnology), or 10 µg/mL
493 tetracycline (Gold Biotechnology) as appropriate.

494 **Plasmid construction.** The pJW15-P_{fabA}, and pJW15-P_{fabA}(-19G>A) reporter plasmids were
495 constructed by amplifying the region upstream of *fabA* from -432 bp to +27 bp relative to
496 the annotated transcriptional start site from wild-type MG1655 or Suppressor 1,
497 respectively, using the Overlap-pJW15-*fabA* FP and RP primers (**Table S4**). pJW15 was
498 amplified using primers Overlap-pJW15-*fabA* FP1 and RP1. The pJW15 plasmid was a kind
499 of gift from Dr. Tracy Raivio (University of Alberta) (102, 103). The resulting fragments
500 were assembled using HiFi Assembly master mix (New England Biolabs) as per the
501 manufacturer's instructions.

502 **Growth and Sensitivity Assays.** For EOPs assays, cultures were grown overnight, serially
503 diluted, and plated on the indicated media. For *pgsA* depletion, overnight cultures grown
504 in arabinose were washed and diluted 1:100 into fresh LB with 0.2% glucose or arabinose
505 as indicated and grown to OD_{600}=1 before diluting and plating on media with glucose or
506 arabinose respective, as above. EOPs were incubated at 30 °C unless otherwise indicated.
507 Growth curves were performed at the indicated temperature as has been described (43),
508 except that starting cultures for growth curves were grown to early stationary phase
509 before inoculation of growth curves rather than overnight. For CPRG assays (50), strains
510 were streaked on LB plates supplemented with CPRG (40µg/ml) and IPTG (100 µM)
511 incubated overnight at 30°C.

512 **Suppressor isolation and sequencing.** Serially diluted cultures were spread on LB plates
513 and incubated overnight at 30°C. Colonies that grew at 30°C were isolated and rechecked
514 for cold resistance through EOP and growth curves. The suppressors were subjected to
515 whole-genome sequencing to identify potential suppressor mutations. Genomic DNA was
516 isolated from the parent and suppressors using a DNeasy Blood and Tissue Kit (Qiagen) as
517 per the manufacturer's instructions. Library preparation and Illumina sequencing were
518 performed by the Microbial Genome Sequencing Center (MiGS, Pittsburgh, PA, USA).
519 Briefly, Illumina libraries were prepared and the libraries were sequenced with paired-
520 end 151 bp reads on a NextSeq 2000 platform to a read depth of at least 200 Mbp. To
521 identify variants from the reference genome (GenBank: U00096.3), reads were trimmed
522 to remove adaptors and the *breseq* software (version 0.35.4) was used to call variants
523 (104). Identified mutations were confirmed with Sanger sequencing. The consensus motif
524 of the FabR binding site of *fabA* was determined using Multiple Em for Motif Elicitation
525 (MEME) tool in the MEME Suite based on the sequence of putative FabR binding sites
526 reported by Feng and Cronan (2011) (64, 105, 106). The ability of the identified P_{fabA}
527 mutation to suppress was confirmed by linking the mutant to *zcb*-3059::Tn*10* (107) and
528 transducing to a clean background.

529 **Lux reporter assays.** Overnight cultures of strains harboring the pJW15-P_{fabA} and pJW15-
530 P_{fabA}(-19G>A) plasmids were sub-cultured at (1:100) into 200 µl of fresh LB broth in a black
531 96-well plate. The plate was incubated in a BioTek Synergy H1 plate reader and the OD_{600}
532 and luminescence intensity were recorded every 2.5 min for 6 hours as described in
533 previously (103, 108). Each biological replicate was performed in technical triplicate.

534 **RNA-seq.** Overnight cultures grown at 42°C were subcultured 1:100 into fresh media and
535 incubated at 42 °C until an OD_{600} of 0.4. Then, the cultures were shifted to a 30 °C water
536 bath for 30 minutes. 500 µL of each culture was immediately fixed in the RNAprotect
537 Bacteria Reagent (Qiagen) as per the manufacturer's instructions. RNA was purified using
538 the RNeasy Kit (Qiagen) with on-column DNase digestion following the manufacturer's
539 protocol for gram-negative bacteria. Library preparation, Illumina sequencing, and
540 analysis of differentially expressed genes were performed by MiGS. Briefly, samples were
541 treated with RNase free DNase (Invitrogen) and library preparation was performed with
542 the Stranded Total RNA Prep Ligation with Ribo-Zero Plus Kit (Illumina). Libraries were
543 sequenced with 2x50 bp reads on a NextSeq2000 (Illumina). Demultiplexing, quality
544 control, and adapter trimming carried out using bcl-convert (Illumina, v3.9.3) and
545 bcl2fastq (Illumina). Read mapping and read quantification were performed with HISAT2
546 (109) and the featureCounts tool in Subreader (110), respectively. Descriptive statistics of
547 the RNA-seq read data can be found in **Table S1**. The raw RNA-seq data is available in the
548 Sequence Read Archive database (SRA) (https://www.ncbi.nlm.nih.gov/sra, BioProject ID
549 PRJNA965821; Reviewer Access).

550 Raw read counts were normalized using the Trimmed Mean of M values algorithm in
551 edgeR (111) and converted to counts per million. The Quasi-Linear F-Test function of

552 edgeR was used for differential expression analysis. Normalized read values and for all
553 genes as well as differential expression analysis statistics can be found in **Dataset S3**.
554 KEGG pathway analysis was conducted using the *"kegga"* function of limma (112).
555 Expression of genes differentially expressed (greater than 2-fold change and $p<0.05$) was
556 subjected to principle component analysis, and pathway and enrichment analysis using
557 the EcoCyc Omics Dashboard (112).

558 **Lipid extraction and TLC.** For thin layer chromatography (TLC) experiments, cultures were
559 grown in LB with 1 mCi/mL ^{32}P until OD_{600} of 0.6-0.8 at the indicated temperature. For
560 temperature downshift experiments, cells were grown at 42 ^{o}C until OD_{600} of 0.2 and then
561 transferred to 30 ^{o}C for 2 hours. For lipid extraction, cells were pelleted and resuspended
562 in 0.2 mL of 0.5 M NaCl in 0.1 N HCl. Lipids were extracted by first adding 0.6 mL of
563 chloroform:methanol (1:2) to create a single-phase solution. After vigorous vortexing for
564 30 minutes, 0.2 mL of 0.5 M NaCl in 0.1 N HCl was added to convert the single-phase
565 solution to a two-phase solution. After centrifugation at 20 000 x g for 5 minutes at room
566 temperature, the lower phase was recovered and used for TLC. Approximately 2,000 cpm
567 of phospholipid extract was subjected to TLC analysis using a HPTLC 60 plate (EMD,
568 Gibbstown, NJ)) developed with either solvent 1: chloroform/methanol/acetic acid
569 [60/25/10] (vol/vol/vol) in **Fig. S4A** or by solvent 2:
570 chloroform/methanol/ammonia/water [65/37.5/3/1] (vol/vol/vol/vol) in **Fig. S4B**.
571 Radiolabeled lipids were visualized and quantified using a Phosphoimager Typhoon FLA
572 9500 (GE). Images were processed and quantified using ImageQuant^{TM} software for
573 scanning and analysis. The phospholipid content is expressed as molecular percentage of
574 the total phospholipids (correcting for the two phosphates per molecule of CL).

575 **Phospholipid composition analysis.** Whole cell lipid extracts were isolated as for TLC
576 temperature downshift experiments without radiolabeling. Absolute amounts of CL, PG,
577 and PE were determined in these lipid extracts using liquid chromatography coupled to
578 electrospray ionization mass spectrometry (LC/MS) in an API 4000 mass spectrometer
579 (Sciex, Framingham, MA, USA) using normal phase solvents as previously published (113).
580 The cardiolipin internal standard $(14:0)_4$CL (Avanti Polar Lipids, Alabaster, AL USA) was
581 added to all samples to quantify CL, PG, and PE within a single run. Standard curves
582 containing reference standards of all three phospholipids, $(18:1)_4$CL (Avanti Polar Lipids),
583 $16:0_1 18:1_1$PG and $16:0_1 18:1_1$PE (Cayman Chemicals, Ann Arbor, MI, USA) were used to
584 quantify the nmol/mg protein for each species (**Dataset 1**) as previously described (114).
585 Percentage values were calculated by dividing the absolute value of that species by the
586 sum of individual molecular species of CL, PG, or PE. The identities of CL species were
587 confirmed using tandem mass spectrometry.
588
589
590 **Acknowledgments**
591

We thank members of the Mitchell Lab for productive discussions. We would like to thank Professor Tracy Raivio (University of Alberta) for the kind gift of pJW15 plasmid. This work was funded by the National Institute of Allergy and Infectious Disease under Award Number R01-AI155915 and R01-AI155915-S1 (to A.M.M.), the National Institute of General Medical Sciences under Award Number R01-GM121493 (to M.B.), and Texas A&M University start-up funds (to A.M.M.).

References

1. Nikaido H. Molecular basis of bacterial outer membrane permeability revisited. Microbiology and Molecular Biology Reviews. 2003;67(4):593-656.
2. Silhavy TJ, Kahne D, Walker S. The bacterial cell envelope. Cold Spring Harbor Perspectives in Biology. 2010;2(5).
3. Henderson JC, Zimmerman SM, Crofts AA, Boll JM, Kuhns LG, Herrera CM, Trent MS. The power of asymmetry: Architecture and assembly of the Gram-negative outer membrane lipid bilayer. Annual Review of Microbiology. 2016;70(1):255-78.
4. Berry J, Rajaure M, Pang T, Young R. The spanin complex is essential for lambda lysis. J Bacteriol. 2012;194(20):5667-74.
5. Rojas ER, Billings G, Odermatt PD, Auer GK, Zhu L, Miguel A, et al. The outer membrane is an essential load-bearing element in Gram-negative bacteria. Nature. 2018;559(7715):617-21.
6. Navarro Llorens JM, Tormo A, Martinez-Garcia E. Stationary phase in gram-negative bacteria. FEMS Microbiol Rev. 2010;34(4):476-95.
7. Lugtenberg EJJ, Peters R. Distribution of lipids in cytoplasmic and outer membranes of *Escherichia coli* K12. Biochimica et Biophysica Acta (BBA) - Lipids and Lipid Metabolism. 1976;441(1):38-47.
8. Kamio Y, Nikaido H. Outer membrane of *Salmonella typhimurium*: accessibility of phospholipid head groups to phospholipase c and cyanogen bromide activated dextran in the external medium. Biochemistry. 1976;15(12):2561-70.
9. Bogdanov M, Pyrshev K, Yesylevskyy S, Ryabichko S, Boiko V, Ivanchenko P, et al. Phospholipid distribution in the cytoplasmic membrane of Gram-negative bacteria is highly asymmetric, dynamic, and cell shape-dependent. Science Advances. 2020;6(23):eaaz6333.
10. Benn G, Mikheyeva IV, Inns PG, Forster JC, Ojkic N, Bortolini C, et al. Phase separation in the outer membrane of *Escherichia coli*. Proceedings of the National Academy of Sciences. 2021;118(44):e2112237118.
11. Konovalova A, Silhavy TJ. Outer membrane lipoprotein biogenesis: Lol is not the end. Philosophical Transactions of the Royal Society B: Biological Sciences. 2015;370(1679):20150030.
12. Konovalova A, Kahne DE, Silhavy TJ. Outer Membrane Biogenesis. Annu Rev Microbiol. 2017;71:539-56.

633 13. Lundstedt E, Kahne D, Ruiz N. Assembly and maintenance of lipids at the
634 bacterial outer membrane. Chemical Reviews. 2021;121(9):5098-123.
635 14. John E. Cronan J, Rock CO. Biosynthesis of membrane lipids. EcoSal Plus.
636 2008;3(1).
637 15. Jones NC, Osborn MJ. Translocation of phospholipids between the outer and
638 inner membranes of *Salmonella typhimurium*. Journal of Biological Chemistry.
639 1977;252(20):7405-12.
640 16. Donohue-Rolfe AM, Schaechter M. Translocation of phospholipids from the inner
641 to the outer membrane of *Escherichia coli*. Proceedings of the National Academy of
642 Sciences. 1980;77(4):1867-71.
643 17. Raetz CR, Kantor GD, Nishijima M, Newman KF. Cardiolipin accumulation in the
644 inner and outer membranes of *Escherichia coli* mutants defective in phosphatidylserine
645 synthetase. J Bacteriol. 1979;139(2):544-51.
646 18. Langley KE, Hawrot E, Kennedy EP. Membrane assembly: movement of
647 phosphatidylserine between the cytoplasmic and outer membranes of *Escherichia coli*. J
648 Bacteriol. 1982;152(3):1033-41.
649 19. White DA, Lennarz WJ, Schnaitman CA. Distribution of lipids in the wall and
650 cytoplasmic membrane subfractions of the cell envelope of *Escherichia coli*. Journal of
651 Bacteriology. 1972;109(2):686-90.
652 20. Ishinaga M, Kanamoto R, Kito M. Distribution of phospholipid molecular species
653 in outer and cytoplasmic membranes of *Escherichia coli*. The Journal of Biochemistry.
654 1979;86(1):161-5.
655 21. Davydova L, Bakholdina S, Barkina M, Velansky P, Bogdanov M, Sanina N. Effects
656 of elevated growth temperature and heat shock on the lipid composition of the inner
657 and outer membranes of *Yersinia pseudotuberculosis*. Biochimie. 2016;123:103-9.
658 22. Osborn MJ, Gander JE, Parisi E, Carson J. Mechanism of Assembly of the Outer
659 Membrane of *Salmonella* typhimurium : Isolation and characterization of cytoplasmic
660 and outer membrane. Journal of Biological Chemistry. 1972;247(12):3962-72.
661 23. Raetz CR, Newman KF. Diglyceride kinase mutants of *Escherichia coli*: inner
662 membrane association of 1,2-diglyceride and its relation to synthesis of membrane-
663 derived oligosaccharides. J Bacteriol. 1979;137(2):860-8.
664 24. Bogdanov M. Renovating a double fence with or without notifying the next door
665 and across the street neighbors: why the biogenic cytoplasmic membrane of Gram-
666 negative bacteria display asymmetry? . Emerging Topics in Life Sciences. 2023;7(1):137-
667 50.
668 25. Grimm J, Shi H, Wang W, Mitchell AM, Wingreen NS, Huang KC, Silhavy TJ. The
669 inner membrane protein YhdP modulates the rate of anterograde phospholipid flow in
670 *Escherichia coli*. Proc Natl Acad Sci U S A 2020;117(43):26907-14.
671 26. Malinverni JC, Silhavy TJ. An ABC transport system that maintains lipid
672 asymmetry in the Gram-negative outer membrane. Proceedings of the National
673 Academy of Sciences. 2009;106(19):8009-14.

674 27. Sutterlin HA, Shi H, May KL, Miguel A, Khare S, Huang KC, Silhavy TJ. Disruption
675 of lipid homeostasis in the Gram-negative cell envelope activates a novel cell death
676 pathway. Proceedings of the National Academy of Sciences. 2016;113(11):E1565-E74.
677 28. May KL, Silhavy TJ. The *Escherichia coli* phospholipase PldA regulates outer
678 membrane homeostasis via lipid signaling. mBio. 2018;9(2):e00379-18.
679 29. Tang X, Chang S, Qiao W, Luo Q, Chen Y, Jia Z, et al. Structural insights into outer
680 membrane asymmetry maintenance in Gram-negative bacteria by MlaFEDB. Nat Struct
681 Mol Biol. 2021;28(1):81-91.
682 30. Ruiz N, Davis RM, Kumar S. YhdP, TamB, and YdbH are redundant but essential
683 for growth and lipid homeostasis of the gram-negative outer membrane. mBio.
684 2021;12(6):e02714-21.
685 31. Douglass MV, McLean AB, Trent MS. Absence of YhdP, TamB, and YdbH leads to
686 defects in glycerophospholipid transport and cell morphology in Gram-negative
687 bacteria. PLOS Genetics. 2022;18(2):e1010096.
688 32. Jumper J, Evans R, Pritzel A, Green T, Figurnov M, Ronneberger O, et al. Highly
689 accurate protein structure prediction with AlphaFold. Nature. 2021;596(7873):583-9.
690 33. Varadi M, Anyango S, Deshpande M, Nair S, Natassia C, Yordanova G, et al.
691 AlphaFold Protein Structure Database: massively expanding the structural coverage of
692 protein-sequence space with high-accuracy models. Nucleic Acids Research.
693 2021;50(D1):D439-D44.
694 34. Josts I, Stubenrauch CJ, Vadlamani G, Mosbahi K, Walker D, Lithgow T, Grinter R.
695 The structure of a conserved domain of TamB reveals a hydrophobic β taco fold.
696 Structure. 2017;25(12):1898-906.e5.
697 35. Kumar N, Leonzino M, Hancock-Cerutti W, Horenkamp FA, Li P, Lees JA, et al.
698 VPS13A and VPS13C are lipid transport proteins differentially localized at ER contact
699 sites. Journal of Cell Biology. 2018;217(10):3625-39.
700 36. Valverde DP, Yu S, Boggavarapu V, Kumar N, Lees JA, Walz T, et al. ATG2
701 transports lipids to promote autophagosome biogenesis. J Cell Biol. 2019;218(6):1787-
702 98.
703 37. Otomo T, Maeda S. ATG2A transfers lipids between membranes *in vitro*.
704 Autophagy. 2019;15(11):2031-2.
705 38. Osawa T, Kotani T, Kawaoka T, Hirata E, Suzuki K, Nakatogawa H, et al. Atg2
706 mediates direct lipid transfer between membranes for autophagosome formation. Nat
707 Struct Mol Biol. 2019;26(4):281-8.
708 39. Cooper BF, Clark R, Kudhail A, Bhabha G, Ekiert DC, Khalid S, Isom GL.
709 Phospholipid transport to the bacterial outer membrane through an envelope-spanning
710 bridge. bioRxiv. 2023:2023.10.05.561070.
711 40. Grasekamp KP, Beaud Benyahia B, Taib N, Audrain B, Bardiaux B, Rossez Y, et al.
712 The Mla system of diderm Firmicute *Veillonella parvula* reveals an ancestral
713 transenvelope bridge for phospholipid trafficking. Nature Communications.
714 2023;14(1):7642.

715 41. Sposato D, Mercolino J, Torrini L, Sperandeo P, Lucidi M, Alegiani R, et al.
716 Redundant essentiality of AsmA-like proteins in *Pseudomonas aeruginosa*. mSphere.
717 2024;9(2):e00677-23.
718 42. Mitchell AM, Wang W, Silhavy TJ. Novel Rpos-dependent mechanisms
719 strengthen the envelope permeability barrier during stationary phase. J Bacteriol.
720 2017;199(2):e00708-16.
721 43. Mitchell AM, Srikumar T, Silhavy TJ. Cyclic enterobacterial common antigen
722 maintains the outer membrane permeability barrier of *Escherichia coli* in a manner
723 controlled by Yhdp. mBio. 2018;9(4):e01321-18.
724 44. Selkrig J, Mosbahi K, Webb CT, Belousoff MJ, Perry AJ, Wells TJ, et al. Discovery
725 of an archetypal protein transport system in bacterial outer membranes. Nature
726 Structural & Molecular Biology. 2012;19(5):506-10.
727 45. Stubenrauch CJ, Dougan G, Lithgow T, Heinz E. Constraints on lateral gene
728 transfer in promoting fimbrial usher protein diversity and function. Open Biology.
729 2017;7(11):170144.
730 46. Stubenrauch C, Belousoff MJ, Hay ID, Shen H-H, Lillington J, Tuck KL, et al.
731 Effective assembly of fimbriae in *Escherichia coli* depends on the translocation assembly
732 module nanomachine. Nature Microbiology. 2016;1(7):16064.
733 47. Cronan JE. The *Escherichia coli* FadR transcription factor: Too much of a good
734 thing? Mol Microbiol. 2021;115(6):1080-5.
735 48. Nunn WD, Giffin K, Clark D, Cronan JE. Role for *fadR* in unsaturated fatty acid
736 biosynthesis in *Escherichia coli*. Journal of Bacteriology. 1983;154(2):554-60.
737 49. Rai AK, Mitchell AM. Enterobacterial common antigen: Synthesis and function of
738 an enigmatic molecule. mBio. 2020;11(4):e01914-20.
739 50. Paradis-Bleau C, Kritikos G, Orlova K, Typas A, Bernhardt TG. A genome-wide
740 screen for bacterial envelope biogenesis mutants identifies a novel factor involved in
741 cell wall precursor metabolism. PLoS Genet. 2014;10(1):e1004056.
742 51. Ruiz N, Falcone B, Kahne D, Silhavy TJ. Chemical conditionality: a genetic strategy
743 to probe organelle assembly. Cell. 2005;121(2):307-17.
744 52. Nikaido H, Vaara M. Molecular basis of bacterial outer membrane permeability.
745 Microbiol Rev. 1985;49(1):1-32.
746 53. Bishop RE. Structural biology of membrane-intrinsic β-barrel enzymes: Sentinels
747 of the bacterial outer membrane. Biochimica et Biophysica Acta (BBA) - Biomembranes.
748 2008;1778(9):1881-96.
749 54. Rowlett VW, Mallampalli V, Karlstaedt A, Dowhan W, Taegtmeyer H, Margolin W,
750 Vitrac H. Impact of membrane phospholipid slterations in *Escherichia coli* on cellular
751 function and bacterial stress adaptation. J Bacteriol. 2017;199(13).
752 55. Tan BK, Bogdanov M, Zhao J, Dowhan W, Raetz CRH, Guan Z. Discovery of a
753 cardiolipin synthase utilizing phosphatidylethanolamine and phosphatidylglycerol as
754 substrates. Proceedings of the National Academy of Sciences. 2012;109(41):16504-9.

755 56. Pluschke G, Hirota Y, Overath P. Function of phospholipids in *Escherichia coli*.
756 Characterization of a mutant deficient in cardiolipin synthesis. Journal of Biological
757 Chemistry. 1978;253(14):5048-55.
758 57. Nishijima S, Asami Y, Uetake N, Yamagoe S, Ohta A, Shibuya I. Disruption of the
759 *Escherichia coli cls* gene responsible for cardiolipin synthesis. Journal of Bacteriology.
760 1988;170(2):775-80.
761 58. Guo D, Tropp BE. A second *Escherichia coli* protein with CL synthase activity.
762 Biochimica et Biophysica Acta (BBA) - Molecular and Cell Biology of Lipids.
763 2000;1483(2):263-74.
764 59. Kikuchi S, Shibuya I, Matsumoto K. Viability of an *Escherichia coli pgsA* null
765 mutant lacking detectable phosphatidylglycerol and cardiolipin. Journal of Bacteriology.
766 2000;182(2):371-6.
767 60. Suzuki M, Hara H, Matsumoto K. Envelope disorder of *Escherichia coli* cells
768 lacking phosphatidylglycerol. Journal of Bacteriology. 2002;184(19):5418-25.
769 61. Shiba Y, Yokoyama Y, Aono Y, Kiuchi T, Kusaka J, Matsumoto K, Hara H.
770 Activation of the Rcs signal transduction system is responsible for the thermosensitive
771 growth defect of an *Escherichia coli* mutant lacking phosphatidylglycerol and cardiolipin.
772 J Bacteriol. 2004;186(19):6526-35.
773 62. Grabowicz M, Silhavy TJ. Redefining the essential trafficking pathway for outer
774 membrane lipoproteins. Proceedings of the National Academy of Sciences.
775 2017;114(18):4769-74.
776 63. Cronan JE, Jr., Gelmann EP. An estimate of the minimum amount of unsaturated
777 fatty acid required for growth of *Escherichia coli*. J Biol Chem. 1973;248(4):1188-95.
778 64. Feng Y, Cronan JE. Complex binding of the FabR repressor of bacterial
779 unsaturated fatty acid biosynthesis to its cognate promoters. Mol Microbiol.
780 2011;80(1):195-218.
781 65. Feng Y, Cronan JE. *Escherichia coli* unsaturated fatty acid synthesis: Complex
782 transcription of the *fabA* gene and *in vivo* identification of the essential reaction
783 catalyzed by FabB. Journal of Biological Chemistry. 2009;284(43):29526-35.
784 66. Henry MF, Cronan JE. *Escherichia coli* transcription factor that both activates
785 fatty acid synthesis and represses fatty acid degradation. Journal of Molecular Biology.
786 1991;222(4):843-9.
787 67. Henry MF, Cronan JE. A new mechanism of transcriptional regulation: Release of
788 an activator triggered by small molecule binding. Cell. 1992;70(4):671-9.
789 68. Rock CO, Jackowski S. Pathways for the incorporation of exogenous fatty acids
790 into phosphatidylethanolamine in *Escherichia coli*. J Biol Chem. 1985;260(23):12720-4.
791 69. Heath RJ, Rock CO. Roles of the FabA and FabZ β-hydroxyacyl-acyl carrier protein
792 dehydratases in *Escherichia coli* fatty acid biosynthesis. Journal of Biological Chemistry.
793 1996;271(44):27795-801.
794 70. Ostrander DB, Sparagna GC, Amoscato AA, McMillin JB, Dowhan W. Decreased
795 Cardiolipin Synthesis Corresponds with Cytochromec Release in Palmitate-induced
796 Cardiomyocyte Apoptosis. Journal of Biological Chemistry. 2001;276(41):38061-7.

797 71. Lewis RNAH, Zweytick D, Pabst G, Lohner K, McElhaney RN. Calorimetric, X-Ray
798 Diffraction, and Spectroscopic Studies of the Thermotropic Phase Behavior and
799 Organization of Tetramyristoyl Cardiolipin Membranes. Biophysical Journal.
800 2007;92(9):3166-77.
801 72. De Siervo AJ. Alterations in the phospholipid composition of *Escherichia coli* B
802 during growth at different temperatures. J Bacteriol. 1969;100(3):1342-9.
803 73. Bogdanov M, Sun J, Kaback HR, Dowhan W. A Phospholipid Acts as a Chaperone
804 in Assembly of a Membrane Transport Protein. Journal of Biological Chemistry.
805 1996;271(20):11615-8.
806 74. Mitchell AM, Silhavy TJ. Envelope stress responses: balancing damage repair and
807 toxicity. Nature Reviews Microbiology. 2019;17(7):417-28.
808 75. Luevano-Martinez LA, Kowaltowski AJ. Phosphatidylglycerol-derived
809 phospholipids have a universal, domain-crossing role in stress responses. Arch Biochem
810 Biophys. 2015;585:90-7.
811 76. Fernandez M, Paulucci NS, Peppino Margutti M, Biasutti AM, Racagni GE,
812 Villasuso AL, et al. Membrane Rigidity and Phosphatidic Acid (PtdOH) Signal: Two
813 Important Events in Acinetobacter guillouiae SFC 500-1A Exposed to Chromium(VI) and
814 Phenol. Lipids. 2019;54(9):557-70.
815 77. Shibata A, Ikawa K, Shimooka T, Terada H. Significant stabilization of the
816 phosphatidylcholine bilayer structure by incorporation of small amounts of cardiolipin.
817 Biochimica et Biophysica Acta (BBA) - Biomembranes. 1994;1192(1):71-8.
818 78. Boscia AL, Treece BW, Mohammadyani D, Klein-Seetharaman J, Braun AR,
819 Wassenaar TA, et al. X-ray structure, thermodynamics, elastic properties and MD
820 simulations of cardiolipin/dimyristoylphosphatidylcholine mixed membranes. Chemistry
821 and Physics of Lipids. 2014;178:1-10.
822 79. Pennington ER, Fix A, Sullivan EM, Brown DA, Kennedy A, Shaikh SR. Distinct
823 membrane properties are differentially influenced by cardiolipin content and acyl chain
824 composition in biomimetic membranes. Biochimica et Biophysica Acta (BBA) -
825 Biomembranes. 2017;1859(2):257-67.
826 80. Lopes SC, Ivanova G, de Castro B, Gameiro P. Revealing cardiolipins influence in
827 the construction of a significant mitochondrial membrane model. Biochimica et
828 Biophysica Acta (BBA) - Biomembranes. 2018;1860(11):2465-77.
829 81. Marr AG, Ingraham JL. Effect of temperature on the composition of fatty acids in
830 *Escherichia coli*. Journal of Bacteriology. 1962;84(6):1260-7.
831 82. Garwin JL, Klages AL, Cronan JE. Beta-ketoacyl-acyl carrier protein synthase II of
832 *Escherichia coli*. Evidence for function in the thermal regulation of fatty acid synthesis.
833 Journal of Biological Chemistry. 1980;255(8):3263-5.
834 83. de Mendoza D, Klages Ulrich A, Cronan JE. Thermal regulation of membrane
835 fluidity in *Escherichia coli*. Effects of overproduction of beta-ketoacyl-acyl carrier protein
836 synthase I. Journal of Biological Chemistry. 1983;258(4):2098-101.
837 84. Knapp BD, Huang KC. The effects of temperature on cellular physiology. Annual
838 Review of Biophysics. 2022;51(1):499-526.

839 85. Bogdanov M, Umeda M, Dowhan W. Phospholipid-assisted refolding of an
840 integral membrane protein: Minimum structural features for phosphatidylethanolamine
841 to act as a molecular chaperone. Journal of Biological Chemistry. 1999;274(18):12339-
842 45.
843 86. Raetz CR, Whitfield C. Lipopolysaccharide endotoxins. Annu Rev Biochem.
844 2002;71:635-700.
845 87. Conway T, Creecy JP, Maddox SM, Grissom JE, Conkle TL, Shadid TM, et al.
846 Unprecedented high-resolution view of bacterial operon architecture revealed by RNA
847 sequencing. mBio. 2014;5(4):e01442-14.
848 88. Thomason MK, Bischler T, Eisenbart SK, Förstner KU, Zhang A, Herbig A, et al.
849 Global transcriptional start site mapping using differential RNA sequencing reveals novel
850 antisense rnas in *Escherichia coli*. Journal of Bacteriology. 2015;197(1):18-28.
851 89. Adams PP, Baniulyte G, Esnault C, Chegireddy K, Singh N, Monge M, et al.
852 Regulatory roles of *Escherichia coli* 5' UTR and ORF-internal RNAs detected by 3' end
853 mapping. eLife. 2021;10:e62438.
854 90. Karp PD, Ong WK, Paley S, Billington R, Caspi R, Fulcher C, et al. The EcoCyc
855 database. EcoSal Plus. 2018;8(1):10.1128/ecosalplus.ESP-0006-2018.
856 91. Huerta AM, Collado-Vides J. Sigma70 promoters in *Escherichia coli*: specific
857 transcription in dense regions of overlapping promoter-like signals. Journal of Molecular
858 Biology. 2003;333(2):261-78.
859 92. Dowhan W, Bogdanov M. Lipid-dependent membrane protein topogenesis. Annu
860 Rev Biochem. 2009;78:515-40.
861 93. Bogdanov M, Xie J, Heacock P, Dowhan W. To flip or not to flip: lipid-protein
862 charge interactions are a determinant of final membrane protein topology. J Cell Biol.
863 2008;182(5):925-35.
864 94. Bogdanov M, Dowhan W. Lipid-dependent generation of dual topology for a
865 membrane protein. J Biol Chem. 2012;287(45):37939-48.
866 95. Bogdanov M, Dowhan W, Vitrac H. Lipids and topological rules governing
867 membrane protein assembly. Biochim Biophys Acta. 2014;1843(8):1475-88.
868 96. Ramezanifard R, Golubeva YA, Palmer AD, Slauch JM. TamAB is regulated by
869 PhoPQ and functions in outer membrane homeostasis during *Salmonella* pathogenesis. J
870 Bacteriol. 2023;205(10):e0018323.
871 97. Szklarczyk D, Gable AL, Nastou KC, Lyon D, Kirsch R, Pyysalo S, et al. The STRING
872 database in 2021: customizable protein-protein networks, and functional
873 characterization of user-uploaded gene/measurement sets. Nucleic Acids Res.
874 2021;49(D1):D605-d12.
875 98. Grasekamp KP, Beaud B, Taib N, Audrain B, Bardiaux B, Rossez Y, et al. Bridges
876 instead of boats? The Mla system of diderm Firmicute *Veillonella parvula* reveals an
877 ancestral transenvelope core of phospholipid trafficking. bioRxiv.
878 2023:2023.06.30.547184.

879 99. Baba T, Ara T, Hasegawa M, Takai Y, Okumura Y, Baba M, et al. Construction of
880 *Escherichia coli* K-12 in-frame, single-gene knockout mutants: the Keio collection. Mol
881 Syst Biol. 2006;2:2006.0008-2006.0008.
882 100. Silhavy TJ, Berman ML, Enquist LW. Experiments with gene fusions: Cold Spring
883 Harbor Laboratory; 1984.
884 101. Datsenko KA, Wanner BL. One-step inactivation of chromosomal genes in
885 *Escherichia coli* K-12 using PCR products. Proceedings of the National Academy of
886 Sciences. 2000;97(12):6640-5.
887 102. MacRitchie DM, Ward JD, Nevesinjac AZ, Raivio TL. Activation of the Cpx
888 envelope stress response down-regulates expression of several locus of enterocyte
889 effacement-encoded genes in enteropathogenic *Escherichia coli*. Infect Immun.
890 2008;76(4):1465-75.
891 103. Wong JL, Vogt SL, Raivio TL. Using reporter genes and the *Escherichia coli* ASKA
892 overexpression library in screens for regulators of the Gram negative envelope stress
893 response. Methods Mol Biol. 2013;966:337-57.
894 104. Deatherage DE, Barrick JE. Identification of mutations in laboratory-evolved
895 microbes from next-generation sequencing data using breseq. Methods Mol Biol.
896 2014;1151:165-88.
897 105. Bailey TL, Elkan C. Fitting a mixture model by expectation maximization to
898 discover motifs in biopolymers. Proc Int Conf Intell Syst Mol Biol. 1994;2:28-36.
899 106. Bailey TL, Johnson J, Grant CE, Noble WS. The MEME Suite. Nucleic Acids Res.
900 2015;43(W1):W39-49.
901 107. Singer M, Baker TA, Schnitzler G, Deischel SM, Goel M, Dove W, et al. A
902 collection of strains containing genetically linked alternating antibiotic resistance
903 elements for genetic mapping of Escherichia coli. Microbiol Rev. 1989;53(1):1-24.
904 108. Rai AK, Carr JF, Bautista DE, Wang W, Mitchell AM. ElyC and cyclic
905 enterobacterial common antigen regulate synthesis of phosphoglyceride-linked
906 enterobacterial common antigen. mBio. 2021;12(6):e02846-21.
907 109. Kim D, Paggi JM, Park C, Bennett C, Salzberg SL. Graph-based genome alignment
908 and genotyping with HISAT2 and HISAT-genotype. Nature Biotechnology.
909 2019;37(8):907-15.
910 110. Liao Y, Smyth GK, Shi W. featureCounts: an efficient general purpose program for
911 assigning sequence reads to genomic features. Bioinformatics. 2013;30(7):923-30.
912 111. Robinson MD, McCarthy DJ, Smyth GK. edgeR: a Bioconductor package for
913 differential expression analysis of digital gene expression data. Bioinformatics.
914 2009;26(1):139-40.
915 112. Ritchie ME, Phipson B, Wu D, Hu Y, Law CW, Shi W, Smyth GK. limma powers
916 differential expression analyses for RNA-sequencing and microarray studies. Nucleic
917 Acids Research. 2015;43(7):e47-e.
918 113. Sparagna GC, Johnson CA, McCune SA, Moore RL, Murphy RC. Quantitation of
919 cardiolipin molecular species in spontaneously hypertensive heart failure rats using
920 electrospray ionization mass spectrometry. J Lipid Res. 2005;46(6):1196-204.

921 114. Hryc CF, Mallampalli VKPS, Bovshik EI, Azinas S, Fan G, Serysheva II, et al.
922 Structural insights into cardiolipin replacement by phosphatidylglycerol in a cardiolipin-
923 lacking yeast respiratory supercomplex. Nature Communications. 2023;14(1):2783.

924
925

Figures and Tables

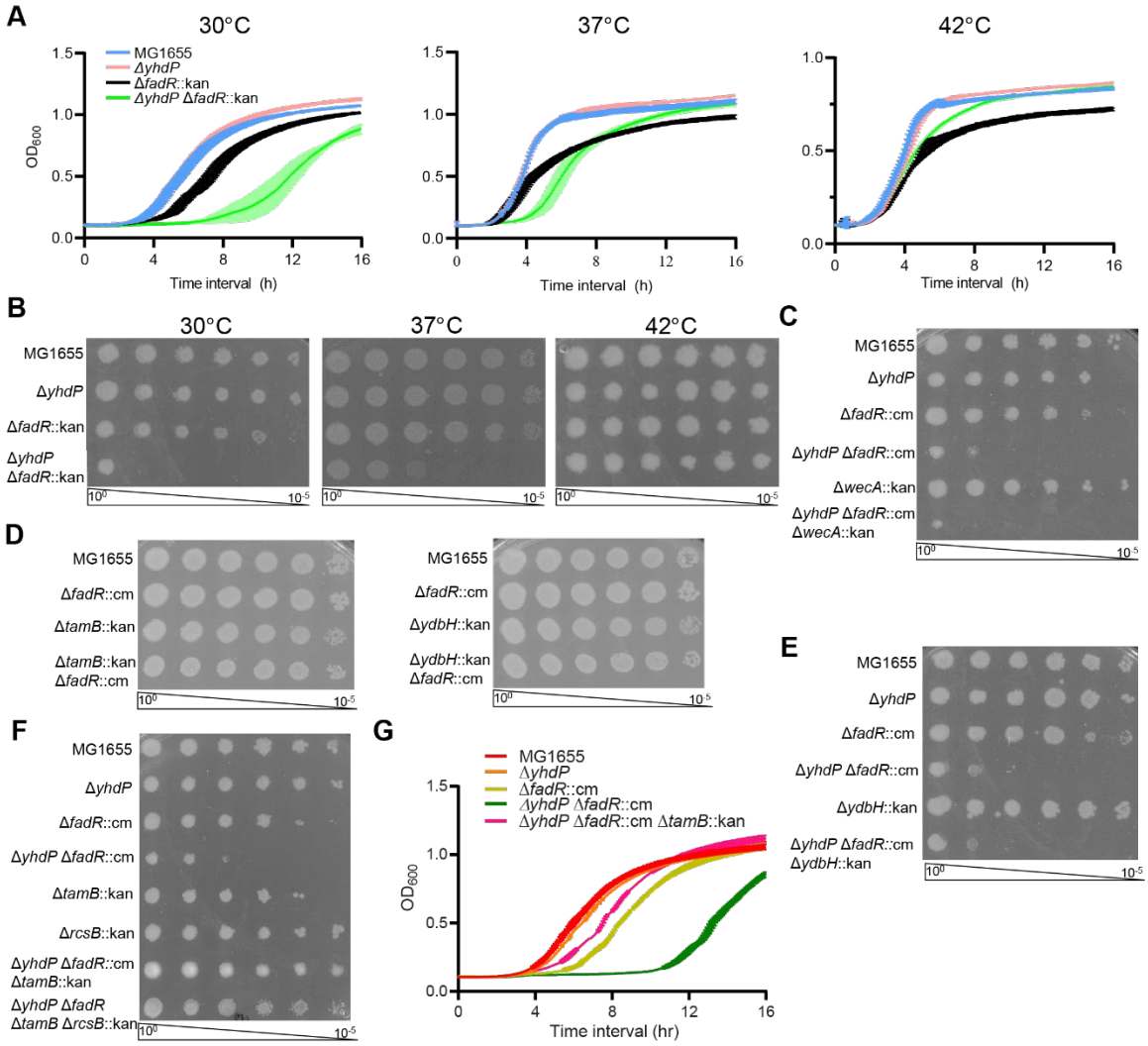

Figure 1. Deletion of *yhdP* and *fadR* causes synthetic cold sensitivity for which TamB is necessary. (A) The Δ*yhdP* Δ*fadR* strain had impaired growth at lower temperatures. **(B)** EOPs were performed to confirm the growth defect of the Δ*yhdP* Δ*fadR* strain. **(C-F)** EOPs were performed at 30 °C to assess cold sensitivity. **(C)** The growth of the Δ*yhdP* Δ*fadR* strain was not affected by the loss of ECA (Δ*wecA*). **(D)** Neither a Δ*tamB* Δ*fadR* strain nor a Δ*ydbH* Δ*fadR* strain exhibited cold sensitivity. **(E)** Deletion of *ydbH* did not suppress cold sensitivity in the Δ*yhdP* Δ*fadR* strain. **(F)** Deletion of *tamB* completely suppressed cold sensitivity in the Δ*yhdP* Δ*fadR* strain and the Rcs stress response was not necessary for this suppression. **(G)** Growth curves were performed at 30 °C . The Δ*yhdP* Δ*fadR* Δ*tamB* strain grew well, indicating suppression was unlikely to result from slow growth.

Quantitative data are shown as the mean of three biological replicates ± the SEM. Images are representative of three independent experiments.

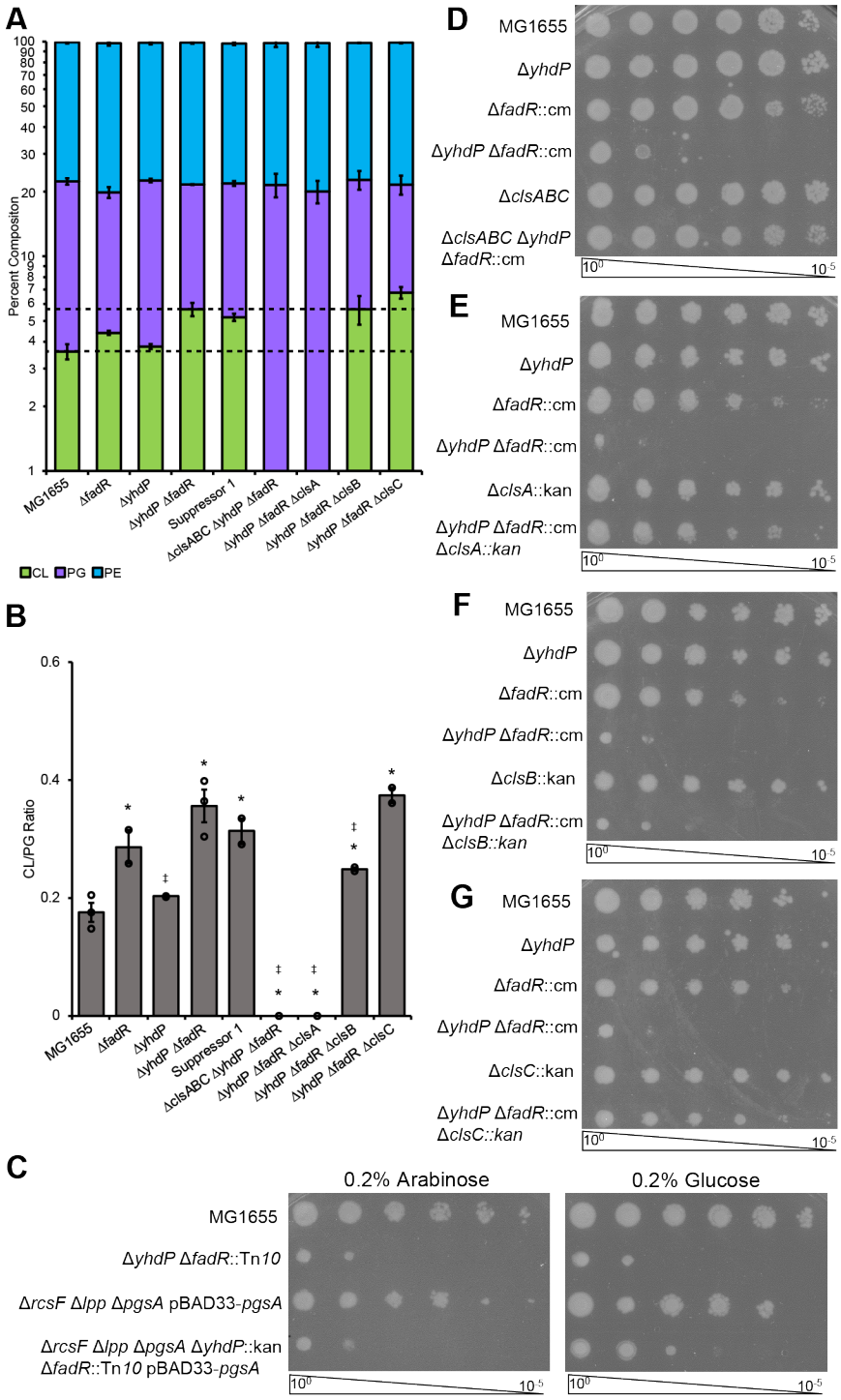

Figure 2. Lowering cardiolipin levels can suppress cold sensitivity of the Δ*yhdP* Δ*fadR* strain. (A-B) Thin layer chromatography (TLC) of lipid extracts was performed for the

947 indicated cultures grown to log phase at 42 °C then transferred to 30 °C for 2 hours before
948 analysis. **(A)** Relative phospholipid levels were calculated. The Δ*yhdP* Δ*fadR* strain shows
949 increased levels of CL and a concomitant decrease in PG levels, increasing the ratio of CL
950 to PG (B). Data are averages of two to three biological replicates ± the SEM. For ratios
951 individual data points are indicated with open circles. * $p<0.05$ vs. MG1655 by Student's
952 T-test; ‡ $p<0.05$ vs. the Δ*yhdP* Δ*fadR* strain by Student's T-test. **(C-G)** Growth effects of
953 altered phospholipid levels were investigated by EOP. Images are representative of three
954 independent experiments. **(C)** PgsA depletion strains in a background where *pgsA* is non-
955 essential were used to assay the effect of lowering PG and CL levels on cold sensitivity.
956 Arabinose induces expression of *pgsA* while glucose represses. Cultures were induced or
957 repressed for 4-5 generations before as well as during the EOP. Lowering PG and CL levels
958 partially suppressed cold sensitivity. **(D)** Deletion of the three CL synthases, *clsA*, *clsB*, and
959 *clsC*, suppressed cold sensitivity of the Δ*yhdP* Δ*fadR* strain. **(E)** Deletion of *clsA* also
960 suppressed cold sensitivity. **(F)** Deletion of *clsB* does not suppress cold sensitivity, while
961 deletion of *clsC* (F) does.
962
963

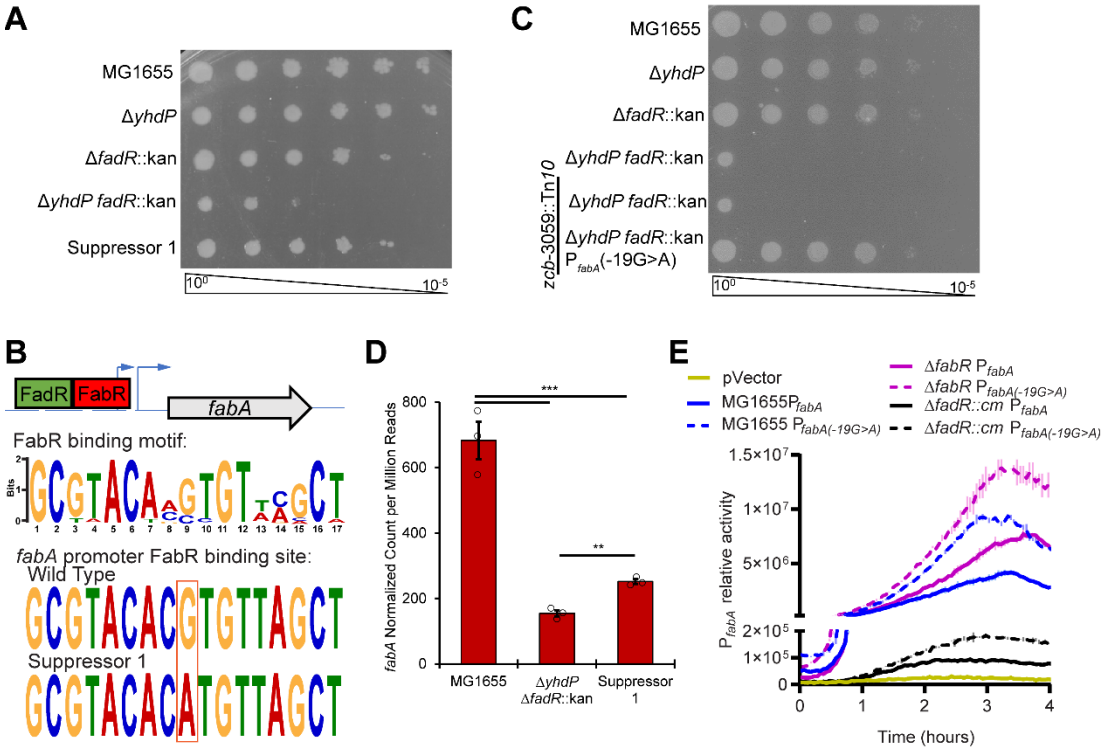

964
965 **Figure 3. Cold sensitivity can be suppressed by increasing *fabA* expression. (A)** The cold
966 sensitivity of a spontaneous suppressor of Δ*yhdP* Δ*fadR* cold sensitivity was tested by EOP.
967 The suppressor returned growth to the level of the Δ*fadR* mutant. **(B)** A diagram of the
968 promoter region of *fabA* is shown with its transcriptional start sites (blue arrows) and
969 regulator binding sites (boxes). FadR acts as an activator while FabR acts as a repressor.
970 The motif of the FabR binding site, generated using MEME, is shown with the sequences
971 of the parent strain and of Suppressor 1. **(C)** The P_{fabA}(-19G>A) mutation was linked to a
972 Tn*10* and transferred to the Δ*yhdP* Δ*fadR* strain by transduction. The Δ*yhdP* Δ*fadR* strain
973 with P_{fabA}(-19G>A) was not cold sensitivity, confirming suppression. **(D)** *fabA* RNA levels
974 are shown. Bars are the mean of three biological replicates ± the SEM. Individual data
975 points are shown as open circles. ** $p<0.005$, *** $p<0.0005$ by quasi-linear F-test. Data
976 are from the RNA-seq experiment in Figure 5 and *fabA* data are also shown in Figure 5F.
977 **(E)** Luciferase reporters of wild-type and mutant *fabA* promoter activity were
978 constructed. The mutation caused similar fold increases in P_{fabA} activity in all strain
979 backgrounds, indicating the activity of the second *fabA* promoter and not FabR binding
980 were likely affected by the suppressor mutation. Data are luminescence relative to OD_{600}
981 and are shown as the average of two biological replicates ± the SEM.
982

983

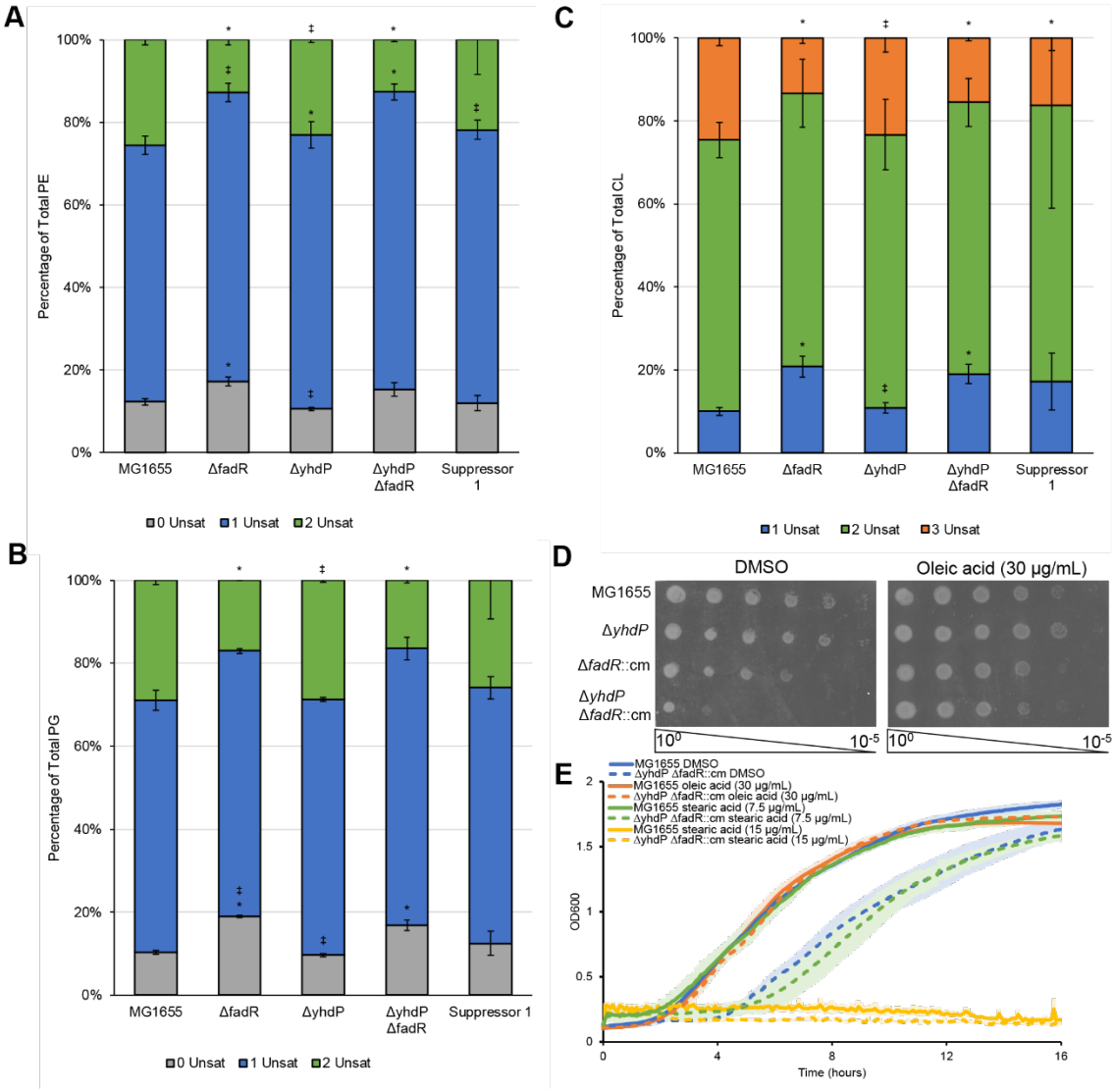

984

985 **Figure 4. Decreasing fatty acid saturation suppresses Δ*yhdP* Δ*fadR* cold sensitivity. (A-**
986 **C)** Lipid were extracted from cells grown to OD_{600} 0.2 at 42 °C then shifted to 30 °C for 2
987 hours before harvest. LC/MS was performed on lipid extracts using absolute
988 quantification and the percentage of each specific species of PE (A), PG (B), and CL (C) was
989 calculated using the sum of all molecular species detected. Suppressor 1 trends towards
990 decreased saturation compared to its parent strain (Δ*yhdP* Δ*fadR*). Data for phospholipids
991 without unsaturations are shown in grey, with one unsaturation in blue, with two
992 unsaturations in green, with three unsaturations in orange. Data are the average of three
993 biological replicates ± the SEM. * $p<0.05$ vs. MG1655 by the Mann-Whitney test; ‡ $p<0.05$
994 vs. the Δ*yhdP* Δ*fadR* strain by the Mann-Whitney test. All molecular species are shown in
995 Fig. S6. **(D)** EOPS were performed on media supplemented with oleic acid or a vehicle
996 control. Oleic acid suppresses the cold sensitivity of the Δ*yhdP* Δ*fadR* strain. **(E)** Growth
997 curves of the indicated strains were performed in the presence of oleic acid, stearic acid,

998 or a vehicle control. Oleic acid suppressed the cold sensitivity of the Δ*yhdP* Δ*fadR* strain
999 while stearic acid did not. Data are the average of three biological replicates ± the SEM.
1000

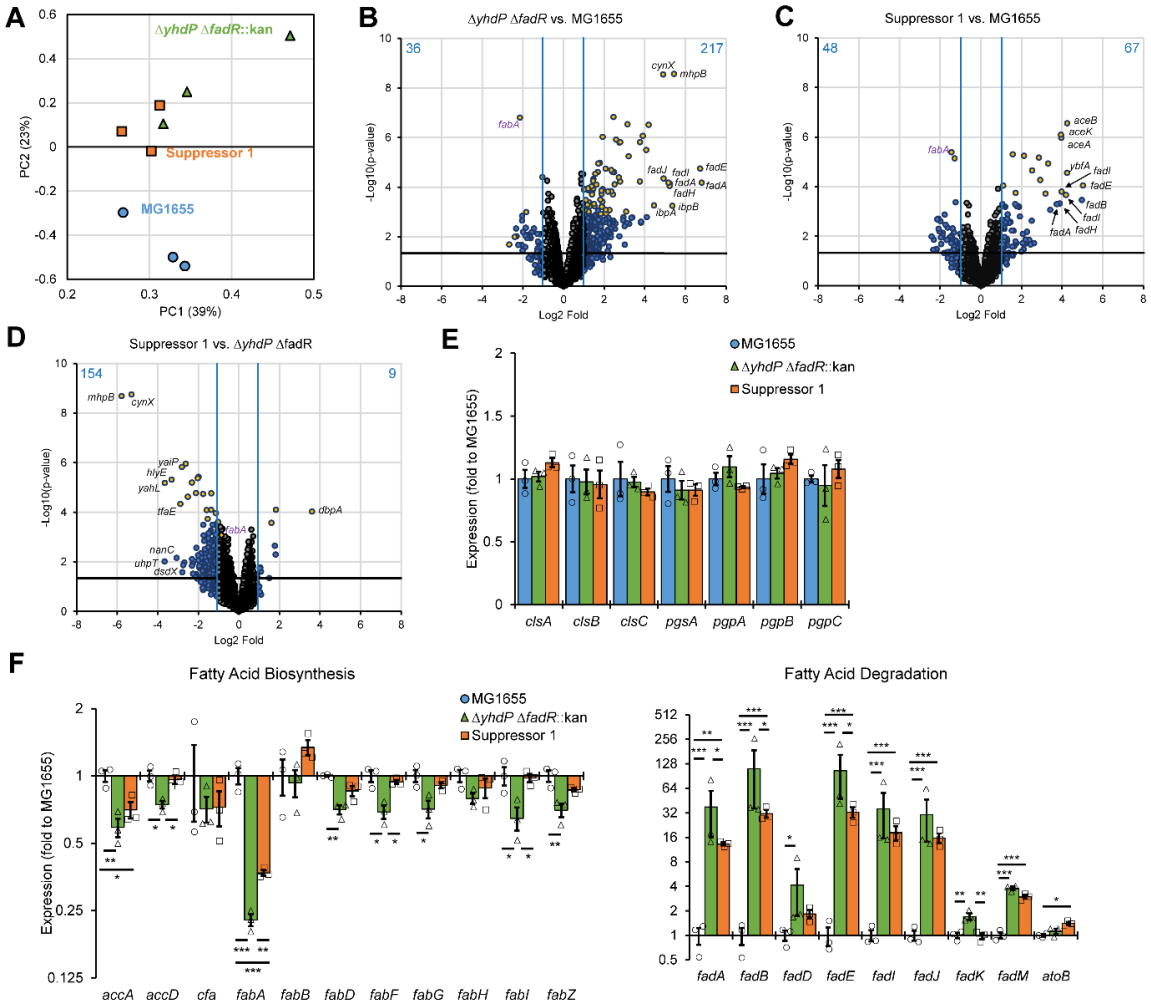

Figure 5. Transcriptional landscape of the Δ*yhdP* Δ*fadR* and suppressed strain. Three biological replicates of the indicated strains were grown at 42 °C to mid-log then transferred to 30 °C for 30 minutes before harvesting RNA and performing RNA-seq. Differential expression was calculated based on a greater than 2-fold change in expression and a p value of less than 0.05 by quasi-linear F-test. **(A)** PCA was performed on the expression of all genes differentially expressed between any groups of samples. Suppressor 1 and the Δ*yhdP* Δ*fadR* strain grouped closer together than to the wild-type strain, although Suppressor 1 was closer to wild type than the Δ*yhdP* Δ*fadR* strain. **(B-D)** Volcano plots show the average fold change and significance of expression changes between the Δ*yhdP* Δ*fadR* strain and wild-type MG1655 (B), Suppressor 1 and wild-type MG1655 (C), and Suppressor 1 and the Δ*yhdP* Δ*fadR* strain (D). Genes with changes greater than 2-fold are shown in blue, while genes with changes less than 2-fold are shown in grey. Genes with a q-value (false discovery rate) of less than 0.05 are shown in yellow. Blue lines indicate a 2-fold change and dotted line indicates p>0.05. The number of up or down regulated genes is indicated in blue. The names of the 10 genes with the largest changes are called out. More genes were up-regulated then down regulated in the Δ*yhdP* Δ*fadR* strain and Suppressor 1 vs. wild type. More genes were down regulated in

1019 Suppressor 1 compared to the Δ*yhdP* Δ*fadR* strain. **(E)** Relative expression of genes in the
1020 CL synthesis pathway is shown as averages ± the SEM and individual data points. No
1021 significant changes were evident. **(F)** Relative expression of genes in the fatty acid
1022 synthesis and degradation pathways is shown as averages ± the SEM and individual data
1023 points. A general normalizing of these pathways occurred in Suppressor 1 compared to
1024 the Δ*yhdP* Δ*fadR* strain; however, the most significant change was in the expression of
1025 *fabA*. * $p<0.05$, ** $p<0.005$, *** $p<0.0005$ by quasi-linear F-test.
1026

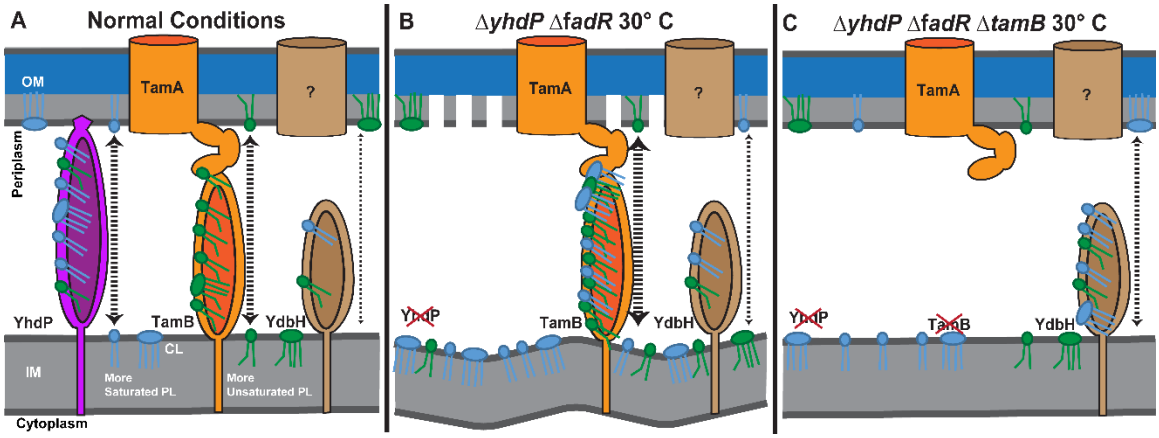

Figure 6. Hypothesized model for the role of YhdP and TamB in phospholipid transport. Our data can be explained by the following model of phospholipid transport. **(A)** In normal conditions, YhdP is mainly responsible for the transport of phospholipids with more saturated fatty acid chains between the IM and OM. TamB shows a strong preference for transporting phospholipids with more unsaturated fatty acids, with YdbH playing a minor role in phospholipid transport. **(B)** In the Δ*yhdP* Δ*fadR* strain, YhdP is not available to transport more saturated phospholipids and the proportion of both saturated fatty acids and cardiolipin is increased, especially at low temperature. The fluidity of the membrane is also lessened by the low temperature. In these conditions, transport of phospholipids between the membranes is impeded, due to clogging of TamB by a combination of less saturated phospholipids and/or bulky and highly disordered CL. This leads to a lethal lack of phospholipids in the OM and overabundance of phospholipids in the IM. **(C)** When *tamB* is deleted in the Δ*yhdP* Δ*fadR* strain, the clogging of TamB is relieved, and the cell relies on YdbH for phospholipid transport overcoming the cold sensitivity. PL: phospholipid